




# PET

(and PET/CT, PET/MR, and SPECT/CT)



Medical Imaging Systems  
DTU, November 2018

Søren Holm




Senior Physicist, ph.d.  
PET- and Cyclotron Unit, Rigshospitalet

1

## Rigshospitalet, Copenhagen

PET





Entrance 39

\$2018

Photo: Flying Professor Andreas Kjær



2





Thanks to:

GE Medical Systems  
CPS Innovation (Bernard Bendriem)  
Siemens Medical Solutions  
Philips Medico  
Impact ([www.impactscan.org](http://www.impactscan.org))  
UC Davis, Simon Cherry

\$2018
3



## Overview (0):

- Different kinds of tomography – PET in particular
- Reconstruction from projections, FBP vs. iterative methods
- Positron imaging history
- Raw data structure - sinograms - types of acquisition and presentation
- 2D/3D, advanced data structure – Michelogram

---

- Resolution and noise
- Scanner physics 1 – PET detectors
- Scanner physics 2 – good, bad, and noise equivalent counts (NEC)
- Attenuation and scatter correction of PET-data
- Hybrid systems – PET/CT- PET/MR - SPECT/CT... Future ideas

\$2018

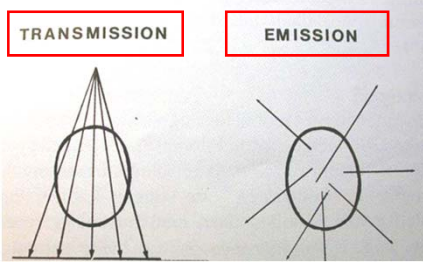
4

**RH** **(T)CT** **ECT** **SPECT** **PET**

Computer(ized)

from:

**TRANSMISSION** **EMISSION**

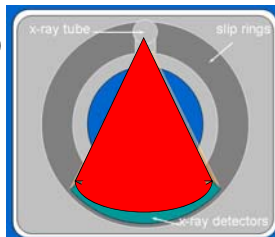


attenuation of photons  
structure / anatomy

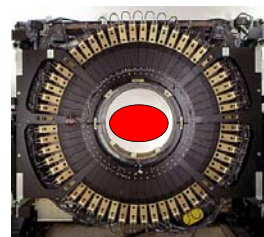
distribution of tracer  
function / physiology

\$2018 5

**RH** **CT** **PET**



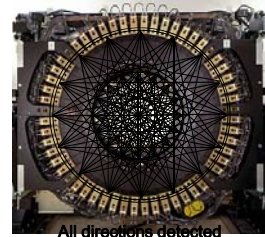
attenuation of photons  
structure / anatomy



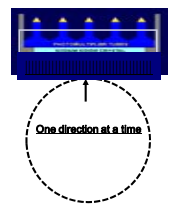
distribution of tracer  
function / physiology

\$2018 6

**RH** PET is stationary – SPECT rotates



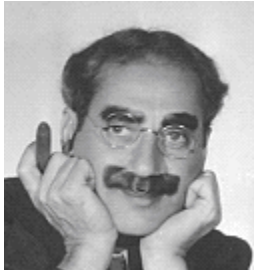
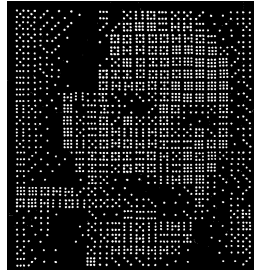
All directions detected  
simultaneously



One direction at a time

\$2018 7

**RH** Radiology Nuclear Medicine

Ken Krowlton, Domino Portraits, 1982

#dots recorded determine what details can be seen in image

And for those ignorants of classic entertainment : this is Groucho Marx  
"I never forget a face, but in your case I'll be glad to make an exception."

\$2018 8



**RH**

# PET is really ART: Annihilation Radiation Tomography


511 keV

$\beta^+$

$e^-$

511 keV

1955



$E = mc^2$

1905

Result: Two photons on an **almost** straight line that **nearly** contains the point of decay

\$2018

13

**RH**

# Positron Emission Tomography (?) or ART

We never detect the positrons directly, only the annihilation photons

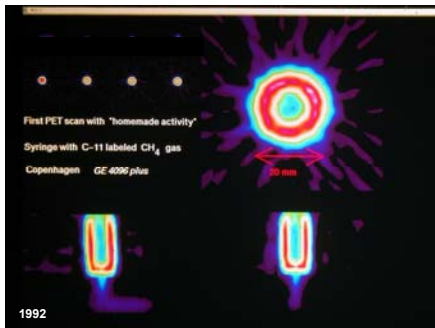
Annihilation Radiation Tomography

First PET scan with "homemade activity"

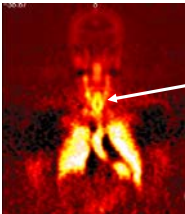
Syringe with C-11 labeled  $CH_4$  gas

Copenhagen GE 4096 plus

1992



20 mm



Inhalation of radioactive  $\beta^+$  gas

\$2018

14

**RH**

# PET radiation detection

A PET scanner counts coincidences

$t_1$

$|t_1 - t_2| < \Delta t?$

yes

coincidence

detector d1

detector d2

Tube or Line Of Response (LOR)

$\Delta t \sim 4-12$  ns

Coincidence window

$\Delta t$

d1

d2

Coincidences

time

\$2018

15

**RH**

# PET detection, Time-of-Flight

A PET scanner counts coincidences

$t_1$

Measure  $t_1 - t_2$

Calculate position along LOR

detector d1

detector d2

Line Of Response (LOR)

$\Delta t = 1$  ns

$\sim \Delta x = 15$  cm

Coincidence window

$\Delta t$

d1

d2

Coincidences

time

\$2018

16

**RH** Time of Flight (TOF) PET  
— more than just a coincidence...

- tried and abandoned in ancient PET times (~1985)
- idea commercially relaunched in 2006 by Philips

$\Delta t$ (ps)	$\Delta d$ (cm)	SNR
100	1.5	5.2
300	4.5	3.0
500	7.5	2.3
600	9.0	2.1

- More information available for image formation
- better image quality, or shorter scanning time, or less injected activity

\$2018 17

**RH** Positron Emitting Isotopes

Isotope	Half-Life	Production
Carbon-11	20.5 min	$^{14}\text{N}(p,\alpha)^{11}\text{C}$
Nitrogen-13	10.0 min	$^{16}\text{O}(p,\alpha)^{13}\text{N}$
Oxygen-15	2.1 min	$^{14}\text{N}(d,n)^{15}\text{O}$
Fluorine-18	110 min	$^{18}\text{O}(p,n)^{18}\text{F}$ (F <sup>-</sup> ), $^{20}\text{Ne}(d,\alpha)^{18}\text{F}$ (F <sub>2</sub> )
Gallium-68	68 min	Daughter of Ge-68 (271 days)
Rubidium-82	1.3 min	Daughter of Sr-82 (25 days)

- Small elements (C,N,O,F) allow “real” biochemistry
- Short half-lives make tracer production an integral part of PET

\$2018 18

**RH** Cyclotrons

Scanditronix 32 MeV

GE Minitrace 11 MeV

\$2018 19

**RH** (small) Cyclotron

**Ion Source**  
Production of  $\text{H}^-$

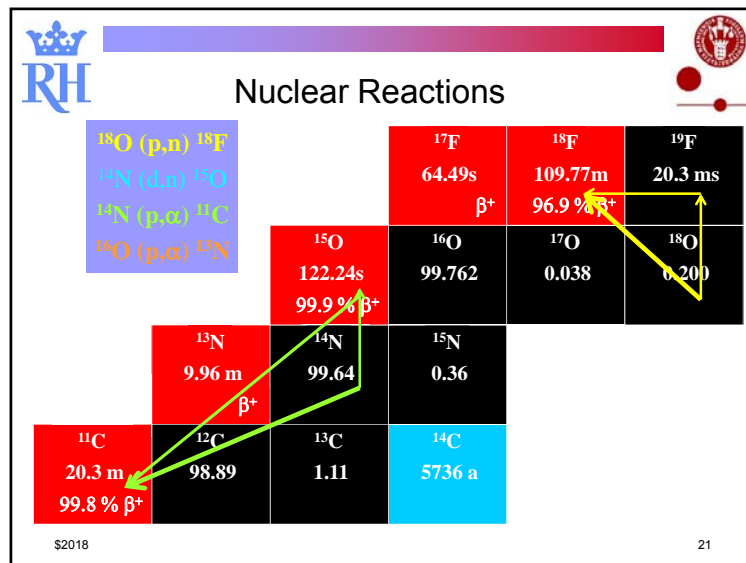
**RF + magnetic field**  
Ion acceleration

**Carbon foil**  
Electron stripping  
 $\text{H}^- \Rightarrow \text{H}^+$  (protons!)

protons do irradiate a

**Target**

\$2018 20



**RH**

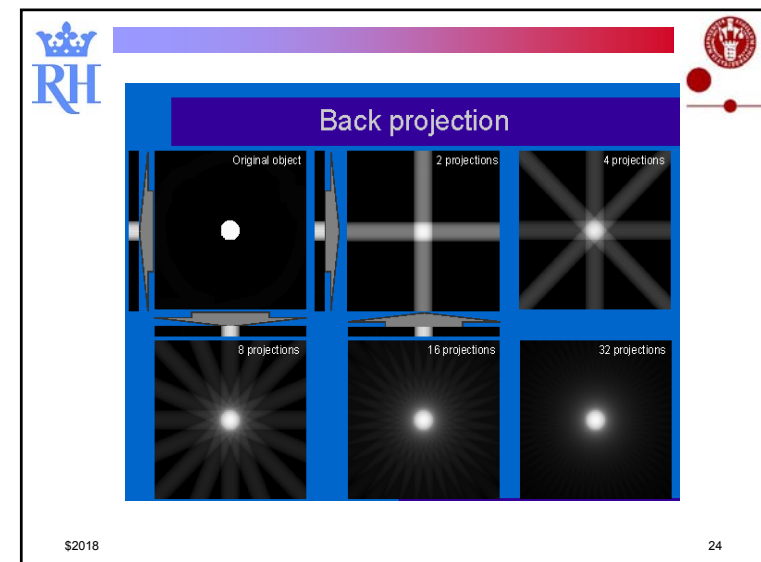
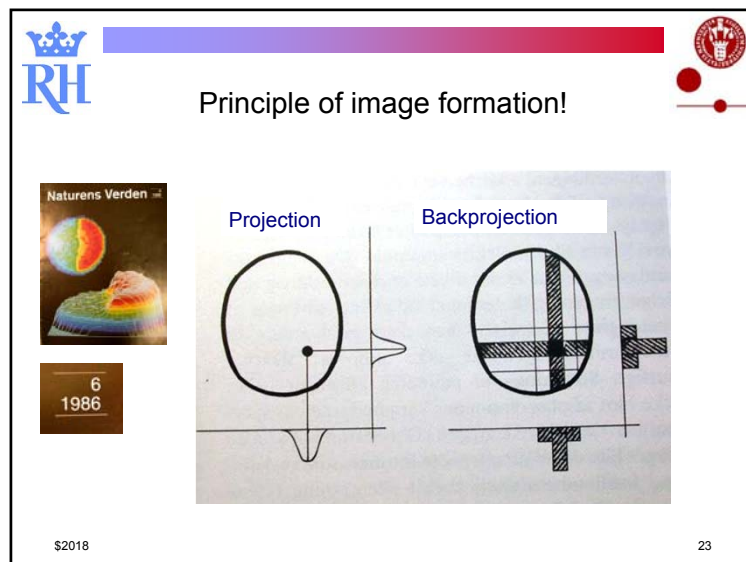
## Overview (1):

- Different kinds of tomography – PET in particular
- Reconstruction from projections, FBP vs. iterative methods
- Positron imaging history
- Raw data structure - sinograms - types of acquisition and presentation
- 2D/3D, advanced data structure – Michelogram

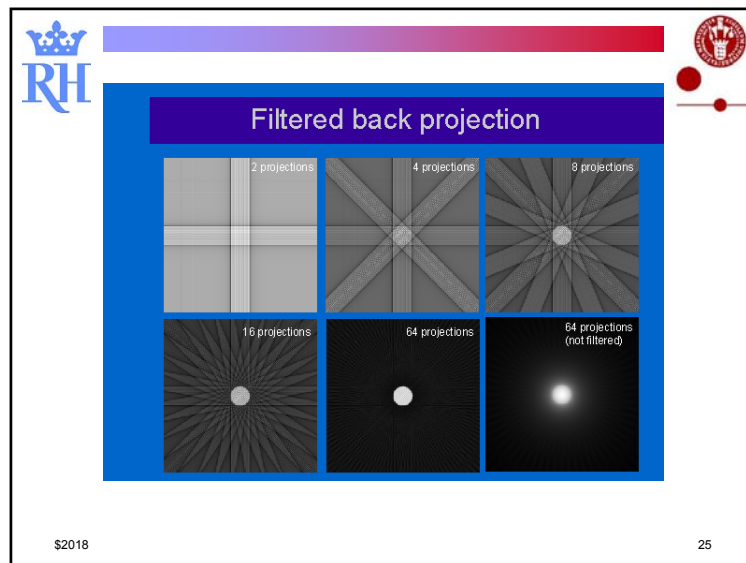
---

- Resolution and noise
- Scanner physics 1 – PET detectors
- Scanner physics 2 – good, bad, and noise equivalent counts (NEC)
- Attenuation and scatter correction of PET-data
- Hybrid systems – PET/CT- PET/MR - SPECT/CT... Future ideas

\$2018 22



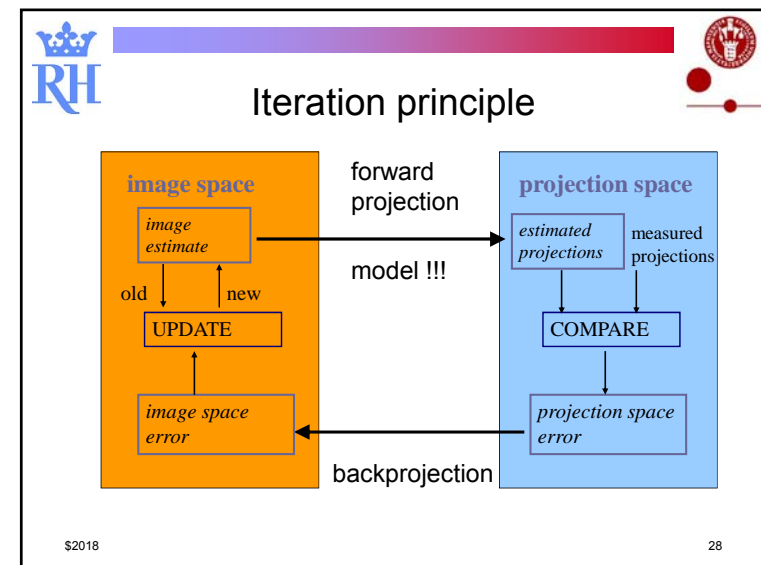
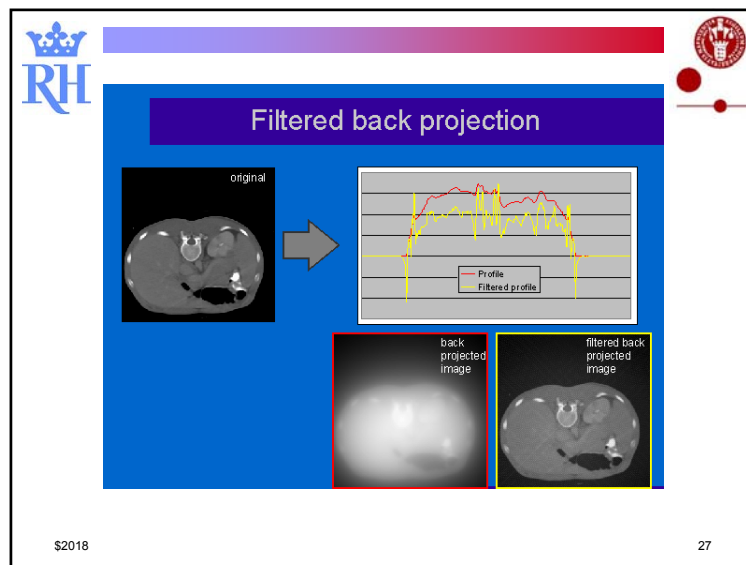


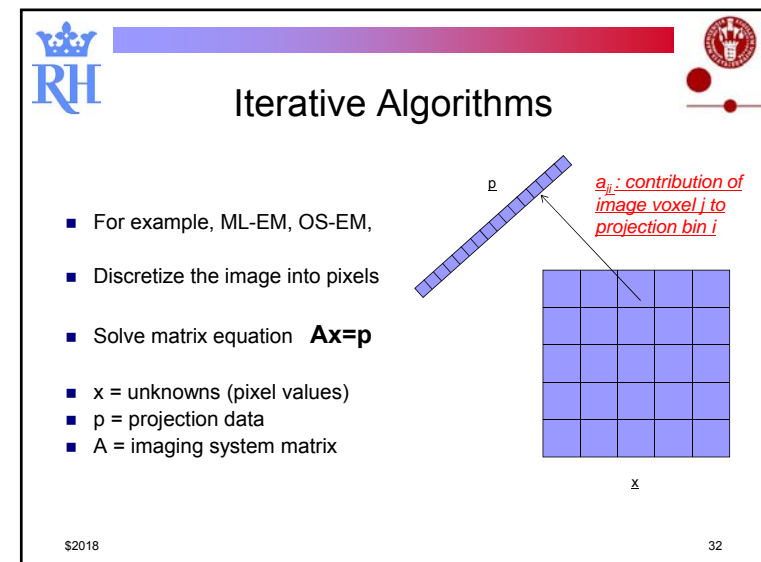
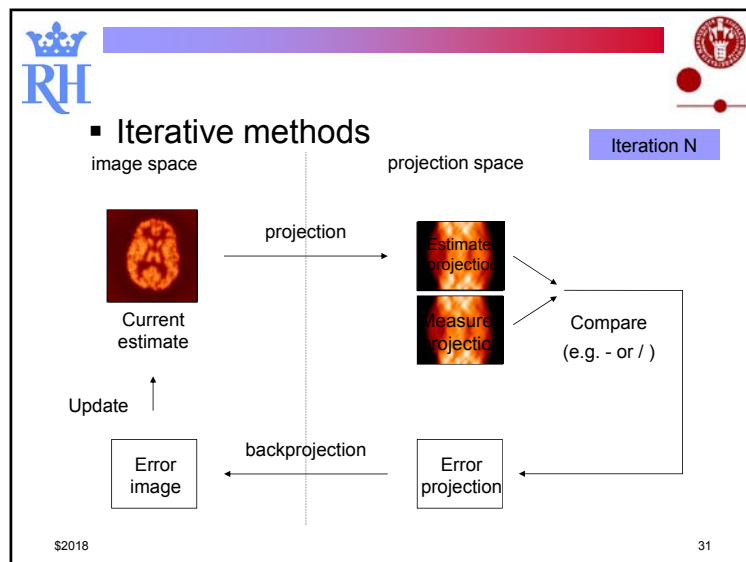
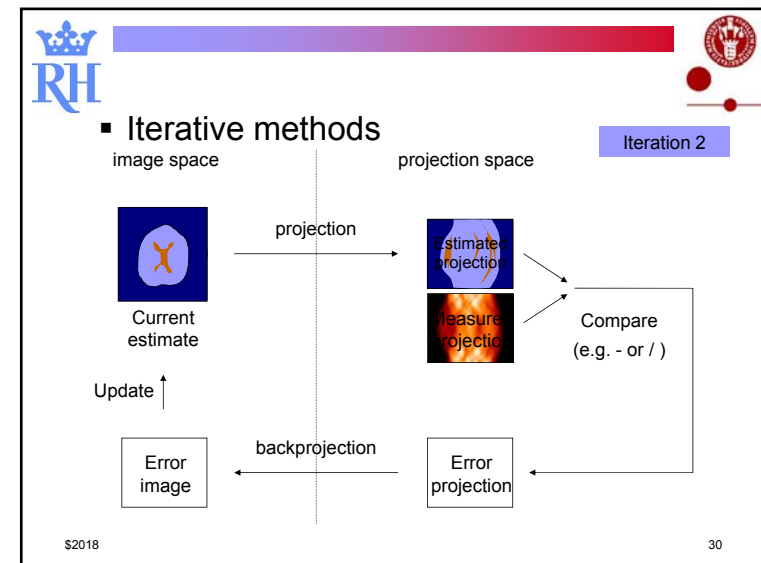
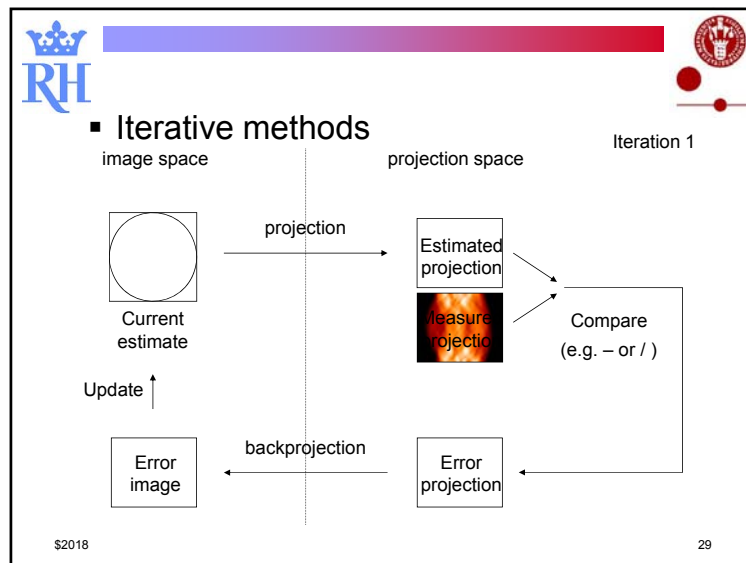


**Example of FBP**  
Filtered Back Projection of X-ray-data (CT)


Institut für Medizinische Physik  
Universität Erlangen-Nürnberg

\$2018 26




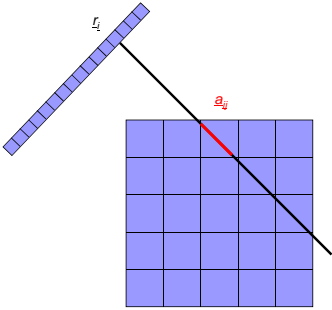






## Line-Length Weighting






Projection (A):

$$r_j = \sum_{i=1}^M a_{ji} x_j$$


Backprojection (A<sup>T</sup>):

$$x_{j,back} = \sum_{i=1}^N a_{ij} r_i$$

\$2018
33




## Iterative Recon versus FBP




	FBP Methods	Iterative Methods
<b>Implementation:</b>	Simple	Complex
<b>Reconstruction speed:</b>	Very fast	Slow with ML-EM, fast with OSEM
<b>Imbedded corrections:</b>	None	anything you can model
<b>Low-count image:</b>	Noisy	Less noise
<b>Reconstruction artifacts:</b>	Streak/spill artifacts	None, regular activity distribution

FBP reconstructed image




\$2018


OSEM reconstructed image



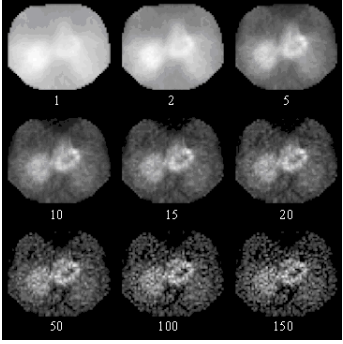
34



## Image at different iteration numbers




Smooth  
Low resolution





Noisy  
High resolution

\$2018
35



## Time to breathe...







[Reykjavik, 25. August 2011\$]


\$2018
36





## Overview (2):







- Different kinds of tomography – PET in particular
- Reconstruction from projections, FBP vs. iterative methods
- Positron imaging history
- Raw data structure - sinograms - types of acquisition and presentation
- 2D/3D, advanced data structure – Michelogram

---

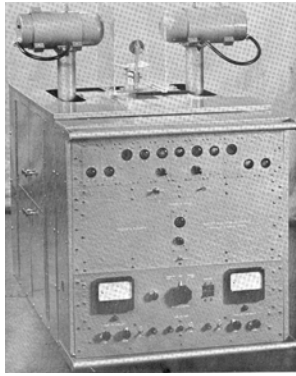
- Resolution and noise
- Scanner physics 1 – PET detectors
- Scanner physics 2 – good, bad, and noise equivalent counts (NEC)
- Attenuation and scatter correction of PET-data
- Hybrid systems – PET/CT- PET/MR - SPECT/CT... Future ideas

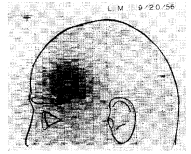
\$2018
37






## Positron scanner (not PET) (Brain tumor scanner at MGH 1955- )






Positrocephalogram (PCG)  
of patient with meningioma

\$2018
38





## COINCIDENCE SCANNING WITH POSITRON-EMITTING ARSENIC OR COPPER IN THE DIAGNOSIS OF FOCAL INTRACRANIAL DISEASE

By  
William H. SWEET, John MEALEY, Jr.,  
Gordon L. BROWNELL and Saul ARONOW

Departments of Surgery and Medicine, Harvard Medical School, and the  
Neurosurgical Service and Physics Research Laboratory of  
Massachusetts General Hospital, Boston, Massachusetts, U.S.A.

### MEDICAL RADIOISOTOPE SCANNING

Proceedings  
of a seminar jointly organized by  
The International Atomic Energy Agency and the World Health Organization  
Vienna, 25 – 27 February, 1959

**Abstract**

This is a report on coincidence counting in man of the paired annihilation gamma rays from positron-emitting copper or arsenic. We discuss the relevant biological behavior of inorganic arsenate and arsenite, of copper versenate, and the results of using these substances during automatic scanning to localize intracranial masses.


Radioscopy of biopsies of the principal normal cephalic tissues, of various types of neoplasms, of hematomas, abscesses and zones of demyelination were carried out. With arsenic the ratios of concentrations of tumor to normal brain were up to 30 for meningiomas. The remaining main tumor types, in order of decreasing concentrations of isotope, were acoustic neuroma, glioblastoma, metastatic malignancy and astrocytoma. The high tumor uptake with arsenic persists long enough so that repeat scans one day after injection are valuable. The muscle: brain ratio of concentrations of circa 3 is high enough to interfere with the accuracy of diagnosis in lesions beneath the lower temporal and especially the upper nuchal masses of muscle. Hematomas, abscesses and zones of demyelination also have high enough ratios to permit localization in the majority of patients. The results on biopsies containing copper versenate showed similar ratios insofar as ascertainable from fewer samples. The meningiomas are a probable exception, yielding lower ratios with the copper.

On the basis of radioscopy both of urinary excretion and of the full range of tissues obtainable at autopsy we compute the local whole-body radiation with  $As^{24}$  to be about 3.2 rads after the usual scanning dose of 2.3 mCi/70 kg. The kidney receives about 12.7 and the liver 9.7 rads. The corresponding figures for  $Cu^{64}$  are 0.325 rads to the whole body, but with a dose to the liver of 3.3 rads because the organ takes up about half of the administered versenate.


The automatic scan includes in 2 simultaneously evolving side views a coincidence count or positrocephalogram (PCG) and a plot of the asymmetry of the total gamma radiation, or asymmetrogramm (AGG). A sagittal PCG is also taken. The lateral scan requires 40 minutes, the sagittal 20 minutes.


Of the more than 9000 scans carried out we report here only the 285 performed in the last 3 1/2 years on a special group of 334 patients, who nearly all proved to have

PCG:  
A "routine"  
examination!



\$2018
39





## Anger camera (Rev.Sci.Instr. 1957)

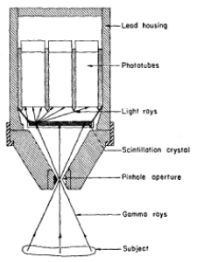


FIG. 1. Sectional drawing of scintillation camera.

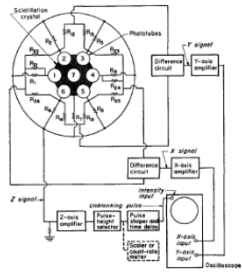




FIG. 2. Block diagram of electronic circuit.

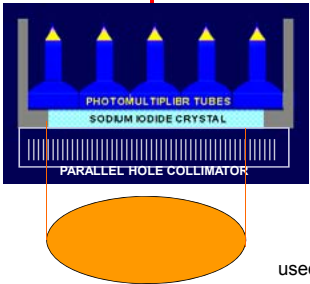
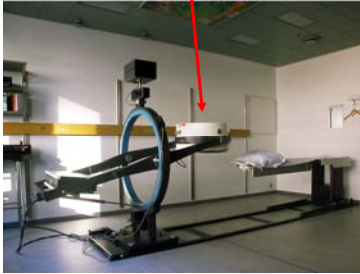
\$2018
40



## Gamma camera principle

position sensitive photon-detector




used for planar imaging or tomography (SPECT)


\$2018


41



## NEW POSITRON TECHNIQUE

The Anger positron camera has proven to be of considerable value in high-sensitivity scanning.<sup>3</sup> This camera, shown in Figure 12, consists of a conventional Anger camera coupled





**NUCLEAR-CHICAGO**


FIGURE 12. Anger positron camera. The crystal matrix is used to select and position pulses from the Anger scintillation camera. (3)

with a second matrix of sodium-iodide detectors. Only pulses in the scintillation camera which are coincident with pulses in the detector matrix are recorded. The position of the pulses are adjusted according to the location of the detector in the second matrix. By a simple control, it is possible to focus on various planes within the object. Because of the very-wide-

Gamma camera for positron imaging:  
NOT a recent invention


\$2018

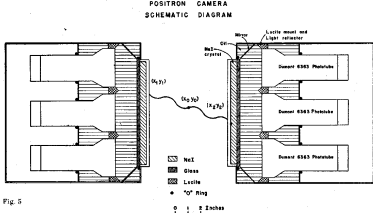
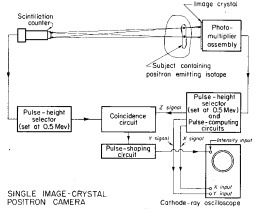
42



## Advances in Dynamic Radioactive Scanning

Compiled and Edited by  
**YEN WANG, M.D., D.Sc. (MED.)**  
Associate Professor of Radiology  
University of Pittsburgh  
and  
Chairman, Department of Radiology  
Homestead Hospital  
Pittsburgh, Pennsylvania




Principles proposed by Hal Anger 1959


\$2018

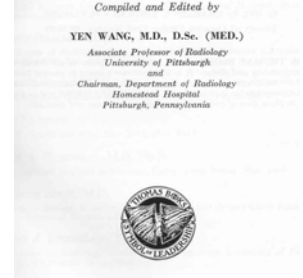
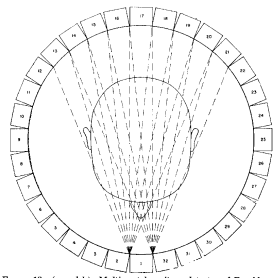
43



## Advances in Dynamic Radioactive Scanning

Compiled and Edited by  
**YEN WANG, M.D., D.Sc. (MED.)**  
Associate Professor of Radiology  
University of Pittsburgh  
and  
Chairman, Department of Radiology  
Homestead Hospital  
Pittsburgh, Pennsylvania



1968 PET

\$2018

44

**PET 1966 -**

Positome I 1966  
32 detectors

Advance 1993  
12096 detectors

HRRT 2002  
119,808 detectors

Therascan 1982  
256 detectors

\$2018

**Special Brain scanner (HRRT)**

119,808  
Detector elements

\$2018

46

**Overview (3):**

- Different kinds of tomography – PET in particular
- Reconstruction from projections, FBP vs. iterative methods
- Positron imaging history
- Raw data structure - sinograms - types of acquisition and presentation
- 2D/3D, advanced data structure – Michelogram

---

- Resolution and noise
- Scanner physics 1 – PET detectors
- Scanner physics 2 – good, bad, and noise equivalent counts (NEC)
- Attenuation and scatter correction of PET-data
- Hybrid systems – PET/CT- PET/MR - SPECT/CT... Future ideas

\$2018

47

**Coincidence Projections**

Detector ring

Coincidence events determine sampling paths (**Lines Of Response**)

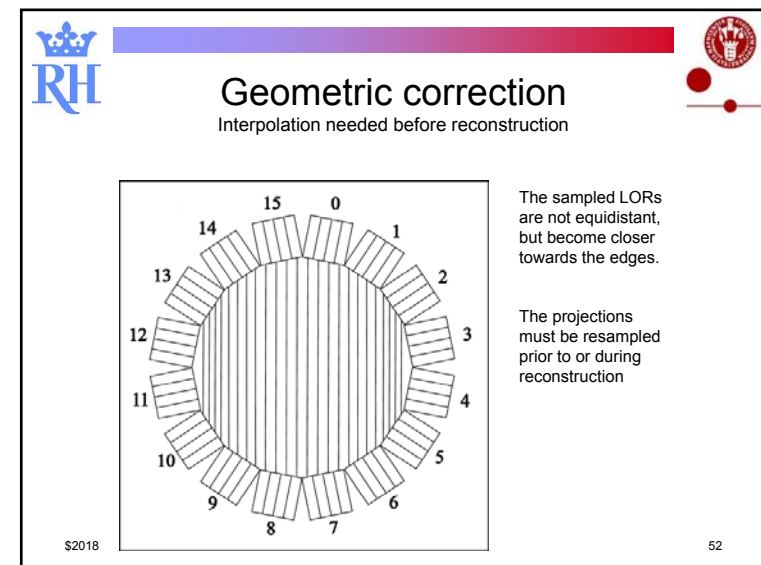
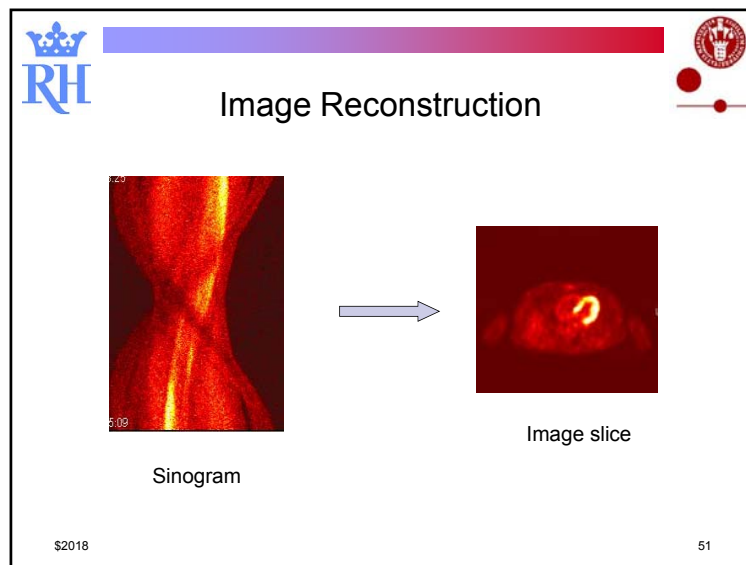
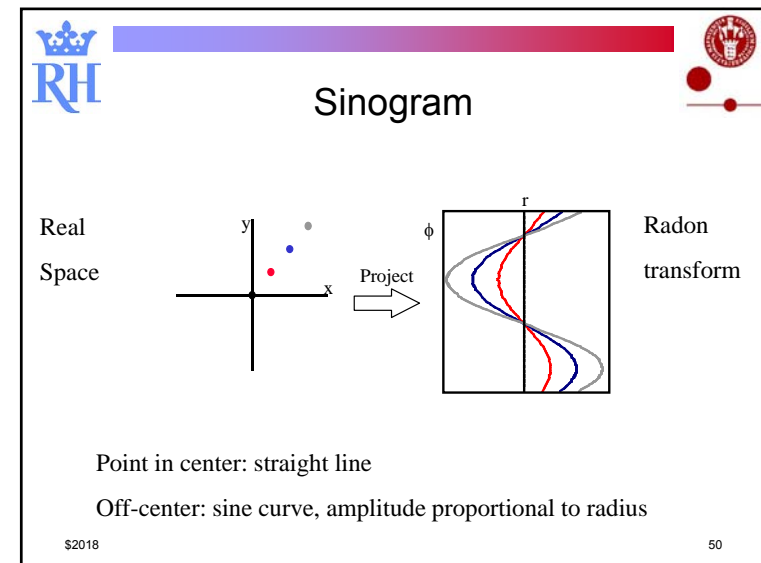
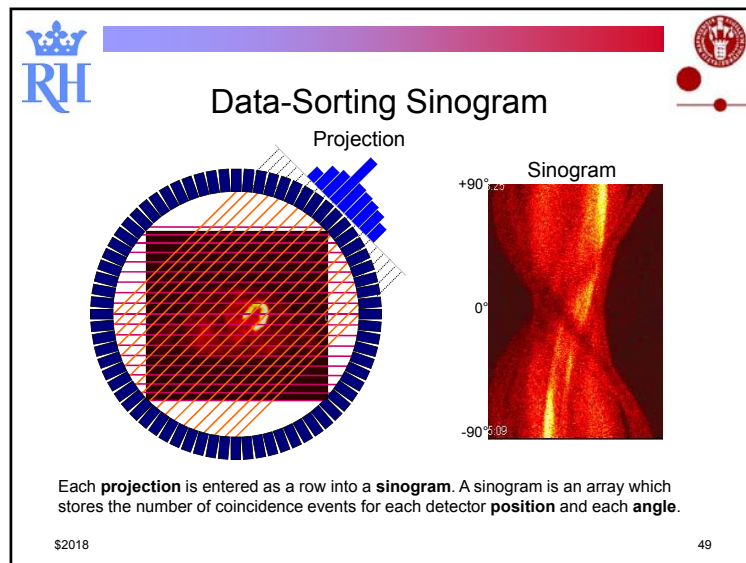
Parallel Lines Of Response are sorted into a row of count numbers (**Projection**), representing the number of 511 keV photon pairs detected.

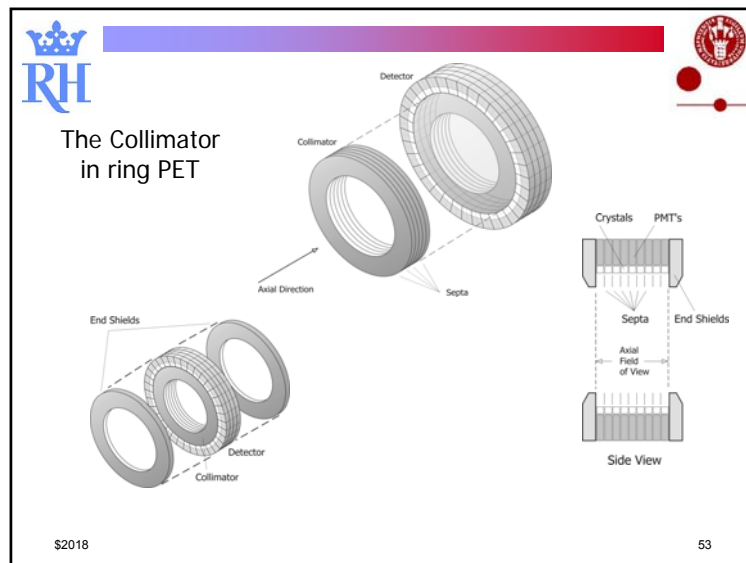
Counts

Projection

\$2018

48





### Static Frame Acquisition

- **Set of slices** in a **single FOV**
- No patient table motion
- Brain scan, tumor spot, heart examinations (myocardial perfusion, metabolism and viability)

The image shows a PET scanner with a patient lying on the table. To the right, four adjacent brain PET static slices are displayed, showing the internal structure of the brain.

Adjacent brain PET static slices

\$2018 54

### Dynamic Frame Acquisition

- **Set of slices over time** in a **single FOV** (like a movie)
- No patient table motion
- Start data acquisition as the tracer is administered
- Quantitative flow study (blood or other fluid): brain or heart

Cerebral dynamic PET scan  
Tracer is  $^{18}\text{F}$ -labeled D2 dopaminergic receptor ligand  
Finding: caudate and putamen normal tracer uptake

A sequence of seven brain PET dynamic frames showing the progression of tracer uptake in the brain over time. The frames are arranged horizontally, with an arrow labeled **time** pointing to the right.

\$2018

### Gated Acquisition

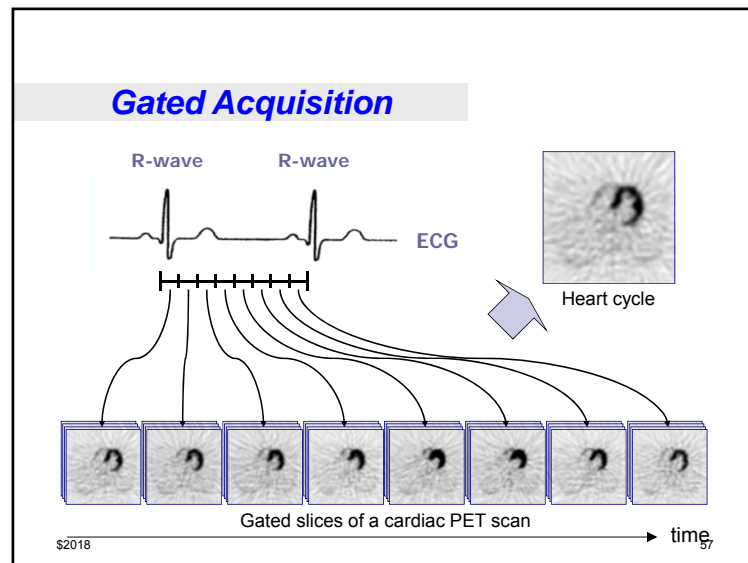
- **Set of slices over time** in a **single FOV** (like a movie)
- No patient table motion
- Heart imaging without cardiac motion blurring
- Myocardial perfusion, metabolism and viability

The image shows a PET scanner with a patient lying on the table. To the right, an electrocardiogram (ECG) trace is displayed, showing the heart's electrical activity over time.

Electrocardiogram

\$2018 56





### List Mode data (LM)

- List mode is an alternative way to store data during acquisition
- In the sinogram, events are counted in each matrix element. In List Mode, the two addresses (the detector numbers) of the two detectors involved are written to a continuous datastream.
- Every millisecond a timestamp is added to the stream
- Signals from cardiac or respiratory monitoring may be added
- After the acquisition, the LM-file can be replayed and sorted into sinograms
- This allows dynamic and gated studies to be acquired without assumptions about time frames and number of gating bins
- In some cases it may even save raw data storage capacity

\$2018 58

### Whole-Body Acquisition

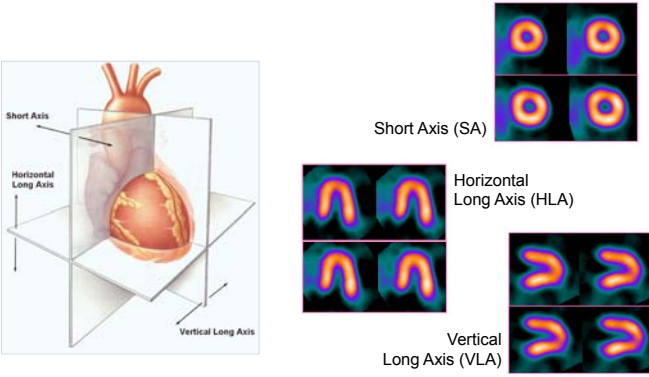
- Set of slices in multiple FOVs
- Step-by-step tabletop motion during acquisition
- Metastatic spread of cancer

The image shows a PET scanner on the left and a whole-body scan on the right. The scan is a vertical image showing the distribution of the tracer throughout the body. The text 'Whole-body scan' is at the bottom right. The text '\$2018' is in the bottom left corner.

### Body Tomographic Planes

The diagram shows a human figure with three planes of tomographic imaging. The Frontal or Coronal plane is shown as a vertical plane. The Transverse or Transaxial plane is shown as a horizontal plane. The Sagittal plane is shown as a vertical plane. The text 'Frontal, Coronal' is at the bottom right. The text '\$2018' is in the bottom left corner.

**RH** Tomographic Planes for the Heart



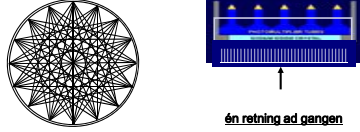
Short Axis (SA)

Horizontal Long Axis (HLA)

Vertical Long Axis (VLA)

\$2018 61

**RH** Comparison of PET and SPECT:



**+ PET**


- 1: Higher sensitivity, with "electronic collimation"
- 2: Fast dynamic scans
- 3: "Biological" tracers with C-11, N-13, O-15, F-18
- 4: Quantitative technique, with attenuation correction

**+ SPECT**

- 1: Dual isotopes possible
- 2: Tc-99m generator + kits !
- 3: Less expensive to run

\$2018 62

**RH** Overview (4):



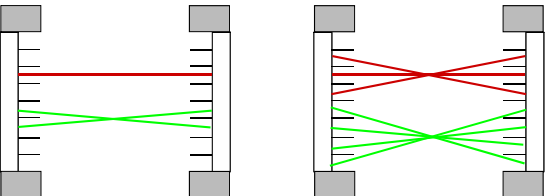
- Different kinds of tomography – PET in particular
- Reconstruction from projections, FBP vs. iterative methods
- Positron imaging history
- Raw data structure - sinograms - types of acquisition and presentation
- 2D/3D, advanced data structure – Michelogram

---

- Resolution and noise
- Scanner physics 1 – PET detectors
- Scanner physics 2 – good, bad, and noise equivalent counts (NEC)
- Attenuation and scatter correction of PET-data
- Hybrid systems – PET/CT- PET/MR - SPECT/CT... Future ideas

\$2018 63

**RH** 2D Imaging



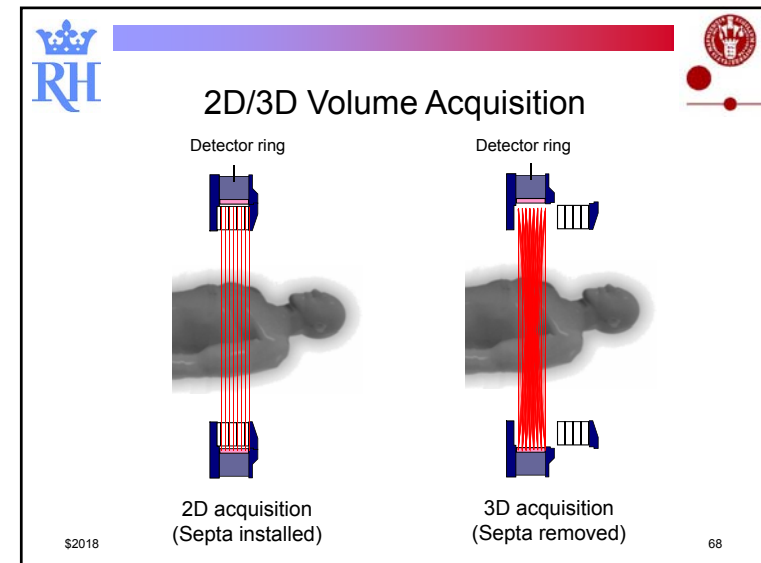
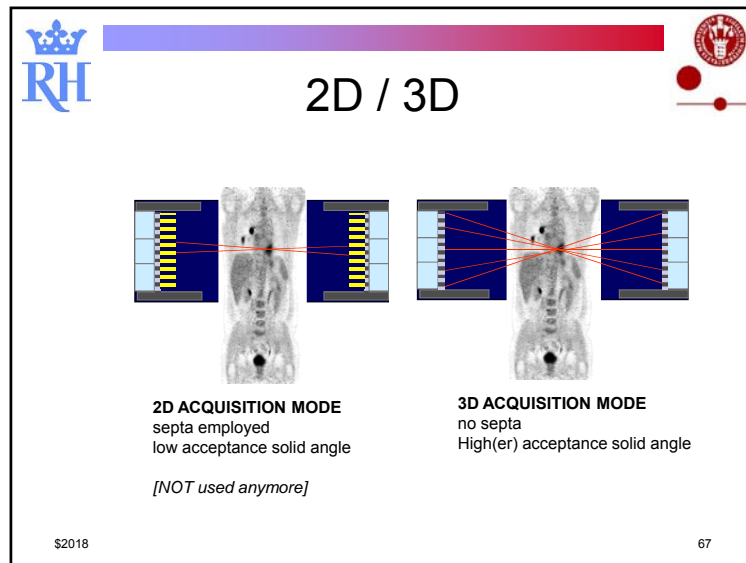
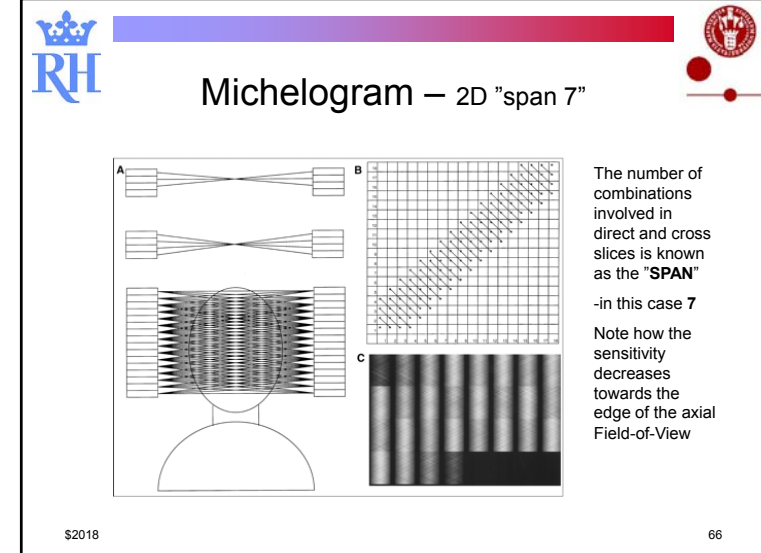
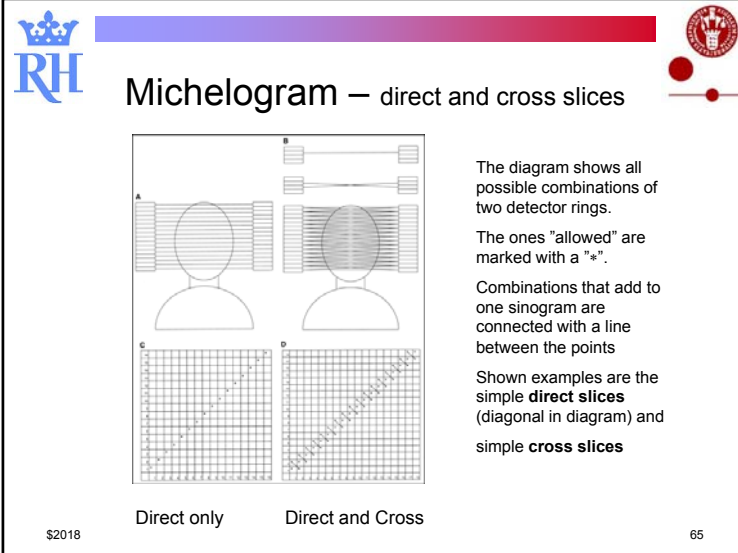
**High Resolution Mode**

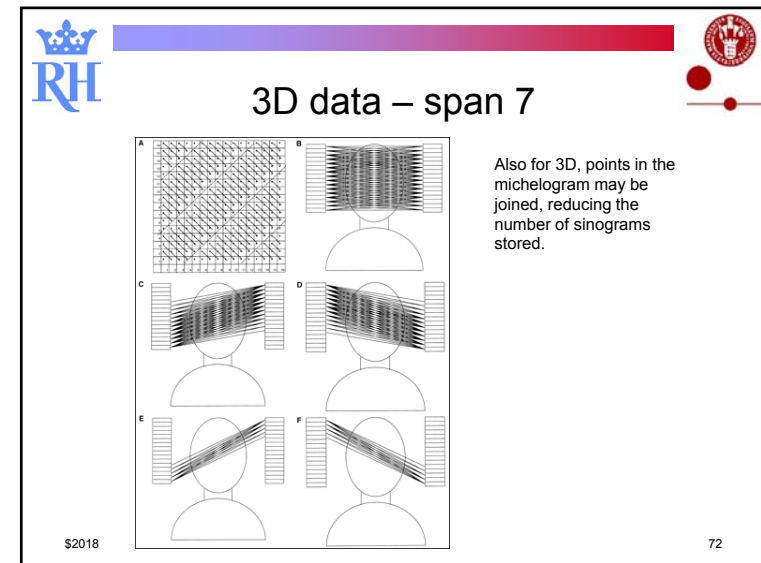
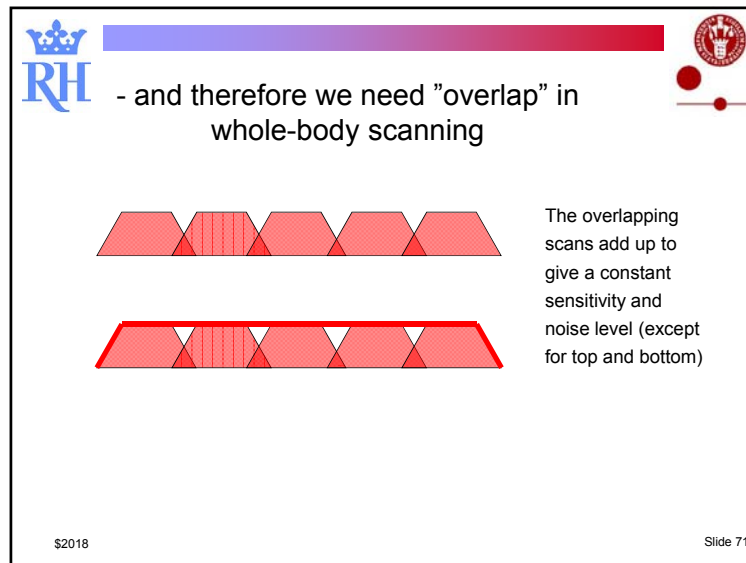
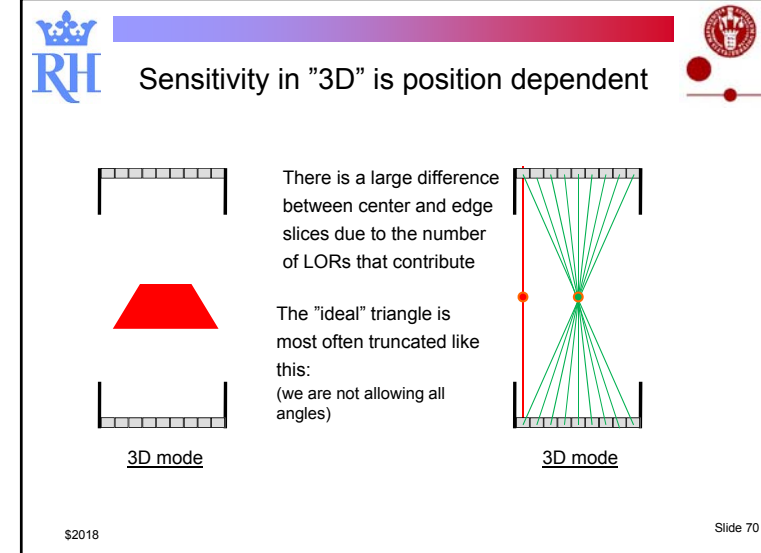
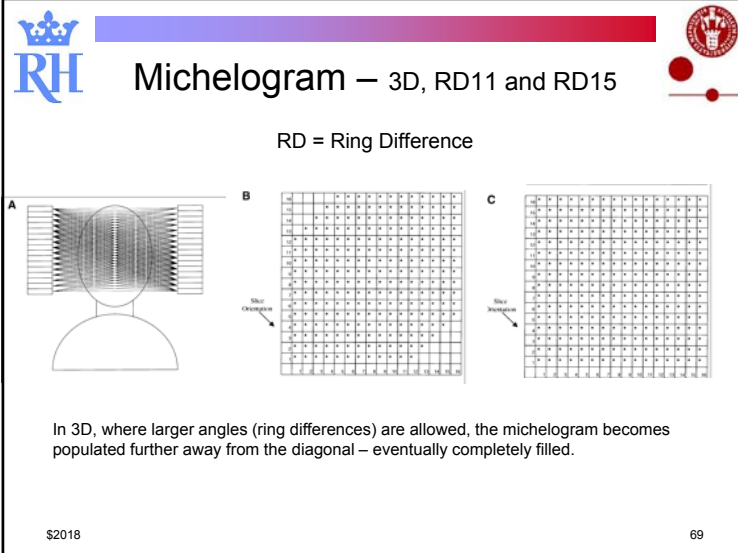
- Direct  $\Delta Z = 0$
- Cross  $\Delta Z = \pm 1$
- Limited Sensitivity



**High Sensitivity Mode**

- Direct  $\Delta Z = 0, \pm 2$
- Cross  $\Delta Z = \pm 1, \pm 3$
- Increased Sensitivity

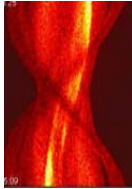
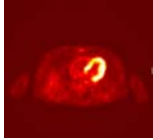
\$2018 64










## Image Reconstruction


→


- Filtered Back-Projection methods:
  - 2D Filtered Back-Projection (2D FBP)
  - 3D Filtered Back-Projection (3D FBP)
- Iterative Reconstruction methods:
  - Maximum Likelihood Expectation Maximization (ML-EM)
  - Ordered Subsets Expectation Maximization (OSEM)
  - Full 3D iteration

\$2018
73







## Overview (5):

- Different kinds of tomography – PET in particular
- Reconstruction from projections, FBP vs. iterative methods
- Positron imaging history
- Raw data structure - sinograms - types of acquisition and presentation
- 2D/3D, advanced data structure – Michelogram

---

- Resolution and noise
- Scanner physics 1 – PET detectors
- Scanner physics 2 – good, bad, and noise equivalent counts (NEC)
- Attenuation and scatter correction of PET-data
- Hybrid systems – PET/CT- PET/MR - SPECT/CT... Future ideas

\$2018
74





## FAQ #1:

What is the smallest *[something]* you can see in a PET scanner?

Wrong question /No simple answer

Depends on the activity concentration/contrast

\$2018
75

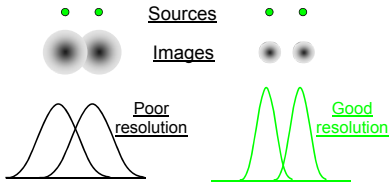


## Spatial Resolution

- ~~How small an object can you see in PET?~~
- Ability to separate two objects close together: **Resolution**

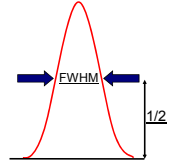
Sources

Images

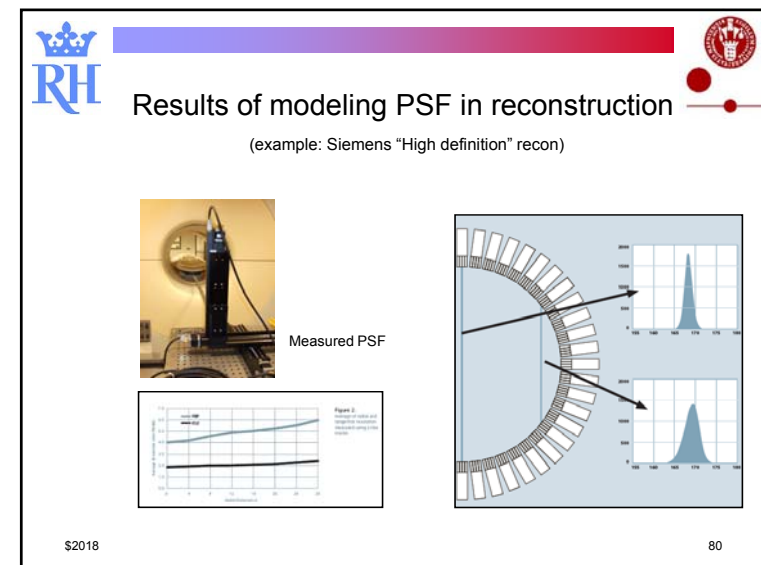
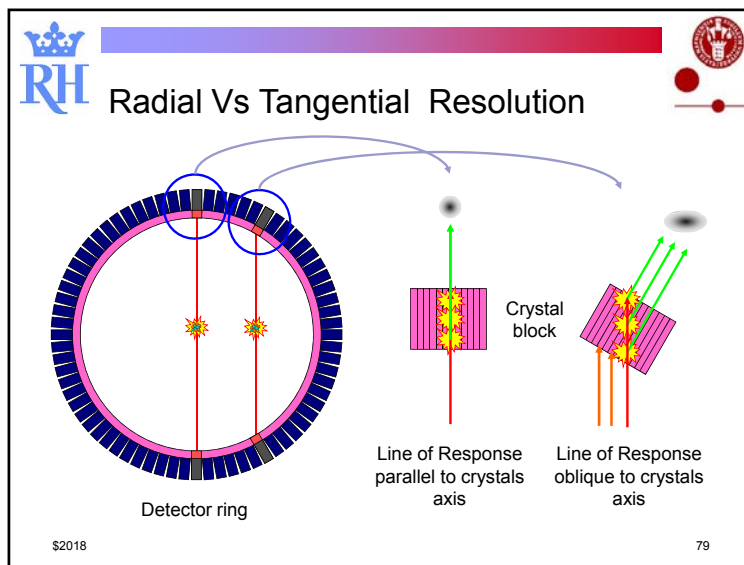
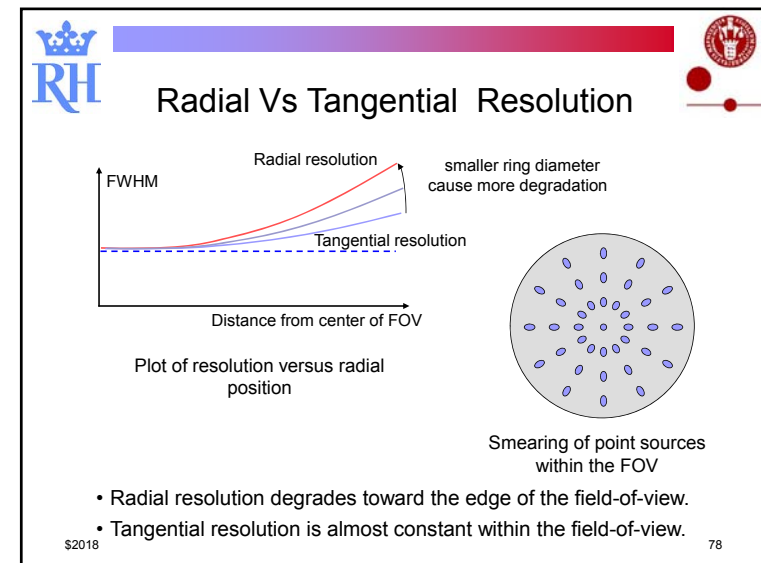
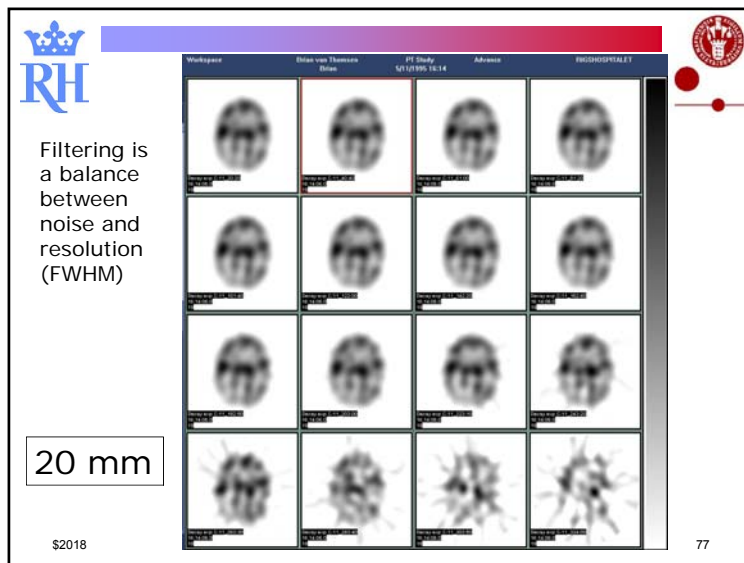


Line profile of a point source (PSF)

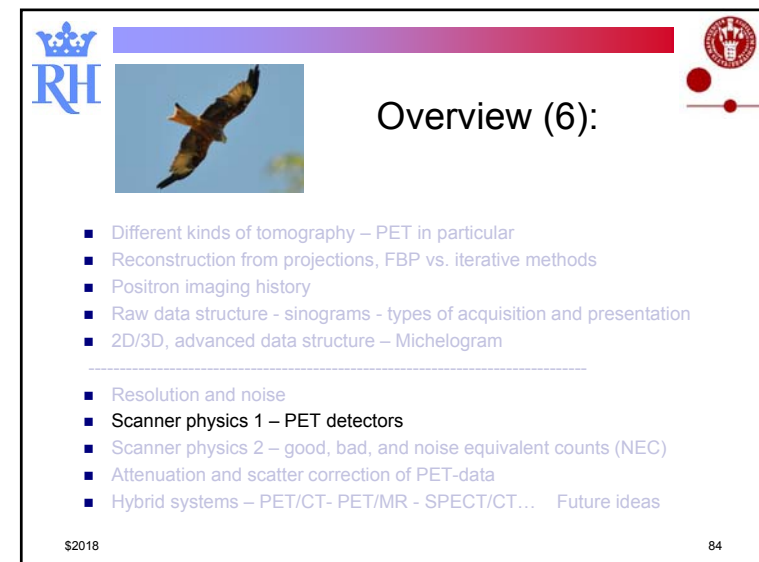
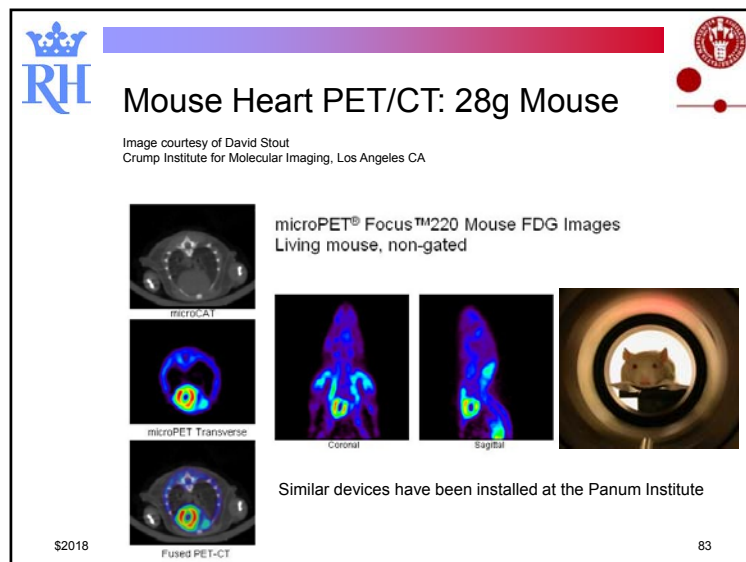
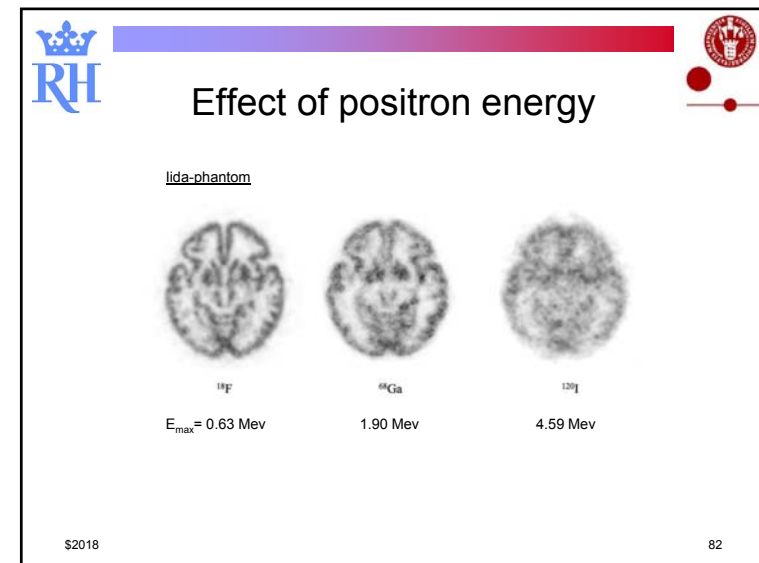
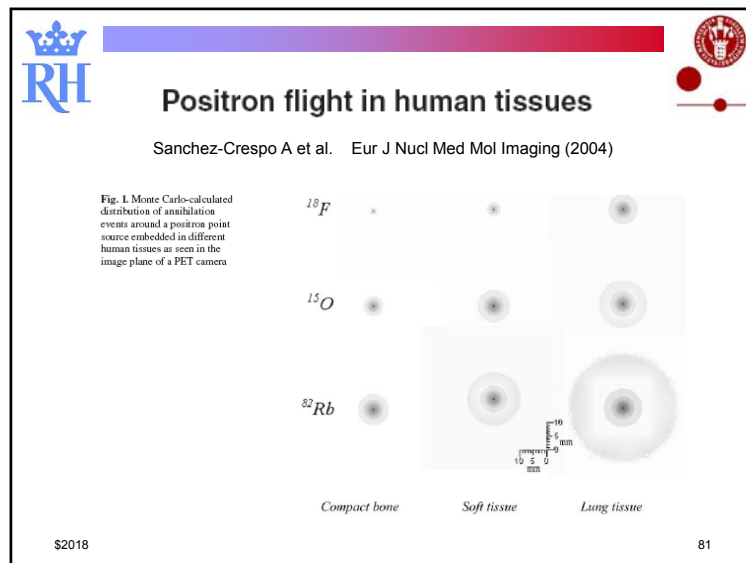
- Full Width at Half Maximum (FWHM) is the measure of resolution (unit: mm).
- Depends on position and direction in the field.
- Typical PET resolution: FWHM  $\approx$  5 mm.



\$2018
76







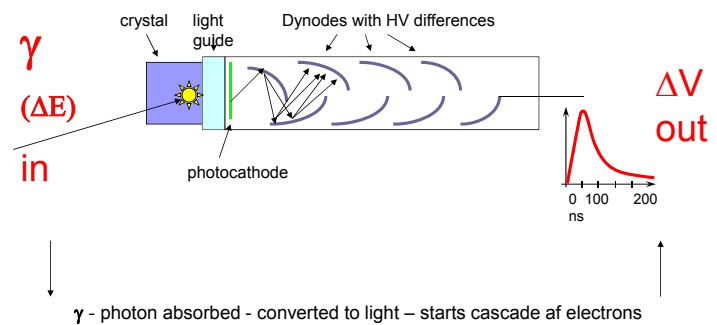
## Detection of 511 keV photons

- First, we need to stop the photons
  - That requires some high Z, high density material
  - which converts the energy to low energy photons
- Then this signal must be amplified and digitized
  - Two options:
    - photo multiplier tube (PMT) or
    - solid state detectors (APD, SiPM)

\$2018

85

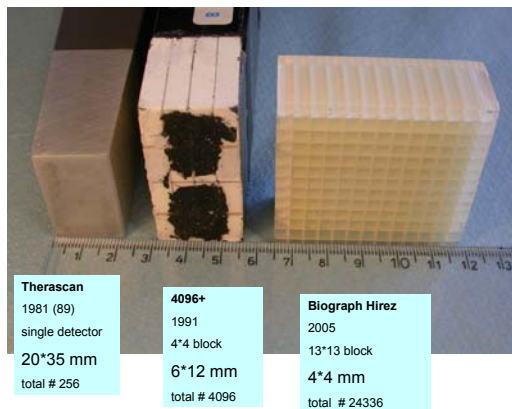
## Scintillation detector



\$2018

86

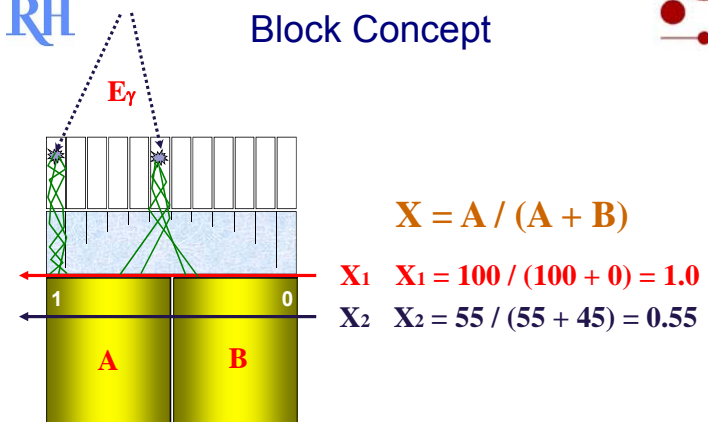
## Evolution of PET-detectors



\$2018

87

## Block Concept



\$2018

88

**RH** Flood Histogram / Position Map

**Anger Logic**

$$X = \frac{A}{A + B}$$

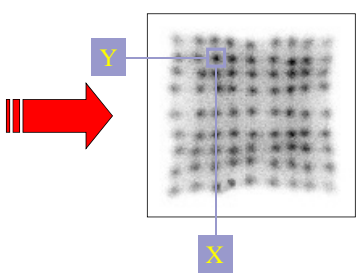
$$Y = \frac{C}{C + D}$$


Diagram illustrating Anger Logic for position determination. A flood histogram (position map) is shown with X and Y axes. A red arrow points from the equations to the histogram.

\$2018 89

**RH** Scintillation detector

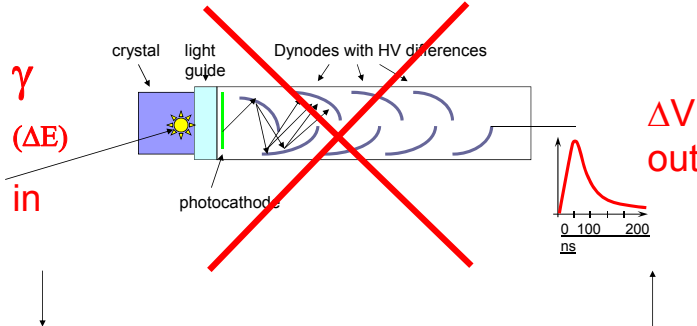


Diagram of a scintillation detector. A  $\gamma$  photon enters from the left, labeled "in". It passes through a crystal, a light guide, and a photocathode. The photocathode is connected to dynodes with HV differences. The output is labeled "out" and shows a pulse shape. A large red X is drawn over the diagram, indicating it is not effective in a magnetic field.

$\gamma$  - photon absorbed - converted to light - starts cascade of electrons

**Not effective in a MAGNETIC FIELD !**

\$2018 90

**RH** Basic PET Detector technologies

Solid-state photo-multipliers (SSPMs) can be fabricated from small silicon sub-pixels to replace PMTs making them attractive for **PET+MR and TOF-PET**:

- fast, low-jitter time response
- magnetic field immunity
- small form-factor

**Technical challenges:**

- Readout circuits/ASIC development
- Multiplexing options
- Handling multi-crystal events
- MR compatible architecture

	PMT	SSPM SiPM	APD
Detection efficiency	25%	50%	50%
Coincidence timing res.	550ps	250ps	1000ps
Gain	$10^6$	$10^5$ - $10^6$	$10^2$
Height	100 mm	2 mm	2 mm
Magnetic Sensitivity	High	Low	Low
Noise	Low	Low	High
Cost	Low	High	High

GE imagination at work

\$2018 91

**RH** "MR-friendly PET detector"

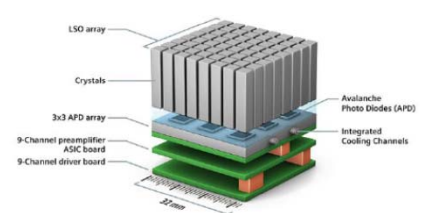


Diagram of an MR-friendly PET detector. It shows a 3x3 array of crystals (LSO array) connected to a 3x3 array of Avalanche Photo Diodes (APD). The APDs are connected to a 9-channel preamplifier ASIC board, which is connected to a 9-channel driver board. Integrated cooling channels are also shown.

\$2018 92

**RH**

# SiPM = Silicon PhotoMultiplier

**SiPM structure**

SiPM is an array of microcells (SPAD's)

Top view

Side view

Single microcell

electrical equivalent circuit of a microcell

Copyright © Hamamatsu Photonics K.K. All Rights Reserved. 8

\$2018 93

**RH**

# Philips Vereos Digital PET dSiPM

First characterization of a digital SiPM based time-of-flight PET detector with 1 mm spatial resolution 2003

Figure 1. Schematic representation of the digital silicon photomultiplier (dSiPM) array. The larger inset depicts a zoom on a single die consisting of four pixels. Each pixel contains 6396 microcells (a number of which are shown in the smaller inset) that are arranged into 4 subpixels.

1 Tile  
16 dies  
4 pixels  
4 subpixels  
~1600 microcells

\$2018 94

**RH**

# DOI measurement with APD

(Depth of Interaction – to avoid parallax-errors)

Presented at EANM 2008 by A. Del Guerra

\$2018 95

**RH**

# Shared PMTs versus 1 to 1 coupling

Analog

Digital 1:1 coupling

Crystal array

Analog PMT

Scintillation photon

DPC tile

Scintillation photon

\$2018 96

**RH** PET Detector Components

Crystal elements and photomultiplier tubes

Detector block

Detector blocks and front-end electronics

Detector ring

Module array

Detector module

\$2018 97

**RH** PET (example: GE Advance)

PMT-gain

Energy-windows

Uniformity

336 \*

Every pair of blocks is tuned for coincidence timing

\$2018 98

**RH** Block contribution to sinogram

A

B

C

All the contributions from a single detector will be on a line, angled as shown. Due to sensitivity differences a certain "rhombic" structure will be visible in the sinogram.

One defective block will show up as a black, empty area in the sinogram

\$2018 99

**RH** Normalisation correction

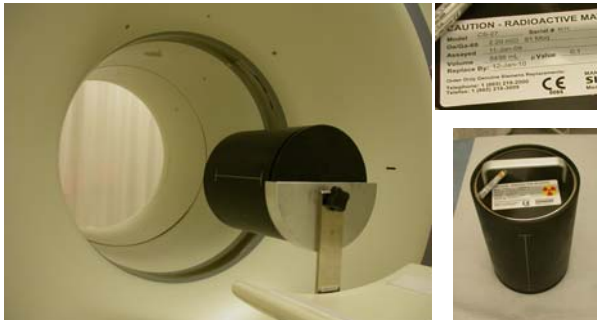
– Compensates systematic efficiency variations (system geometry, crystal efficiency)

Sinogram **before** normalisation correction

Sinogram **after** normalisation correction

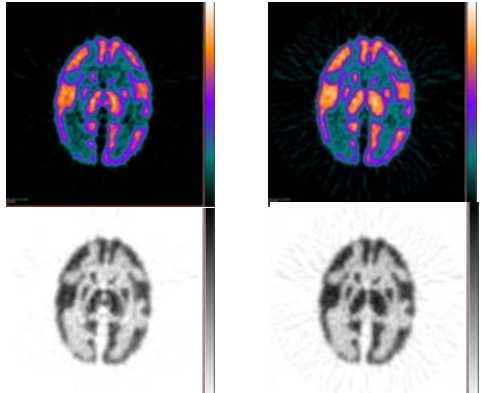
\$2018 100

**RH** Siemens Biograph uses  $^{68}\text{Ge}$  cylinder



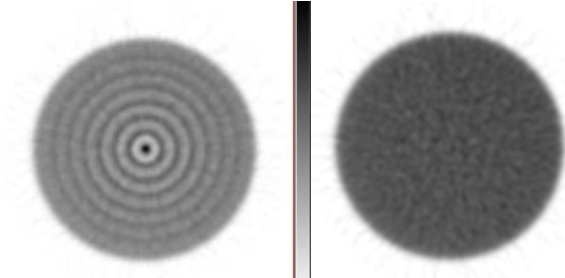
\$2018 101

**RH** Effect of Normalisation



\$2018 102

**RH** Uniform phantom – very sensitive to NORM

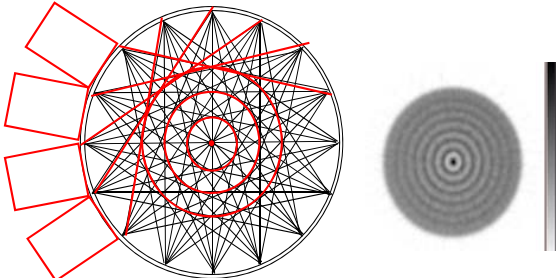


without with

\$2018 103

**RH** Normalisation  
(digression on the origin of ring artefacts)


Red LOR's connect block edges





Lines of Respons (LOR's)

\$2018 104










## Overview (7):


- Different kinds of tomography – PET in particular
- Reconstruction from projections, FBP vs. iterative methods
- Positron imaging history
- Raw data structure - sinograms - types of acquisition and presentation
- 2D/3D, advanced data structure – Michelogram

---

- Resolution and noise
- Scanner physics 1 – PET detectors
- Scanner physics 2 – good, bad, and noise equivalent counts (NEC)
- Attenuation and scatter correction of PET-data
- Hybrid systems – PET/CT- PET/MR - SPECT/CT... Future ideas

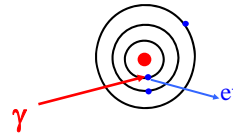
\$2018
105





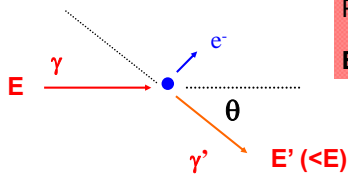
## Two processes stop photons in tissue:

**Absorption:**



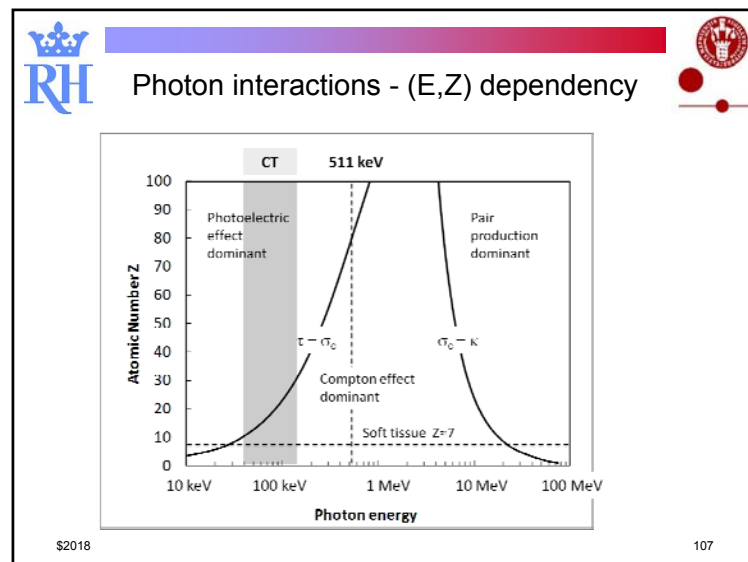
Simple,  
no parameters


**Compton scattering:**




Parameters  
 $E'$  and  $\theta$

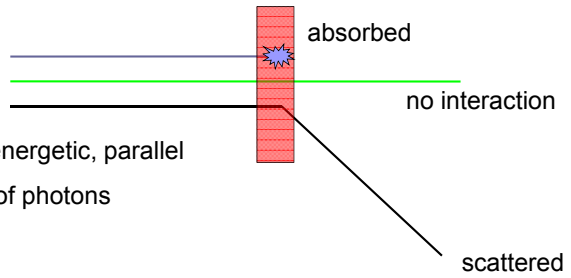
\$2018
106







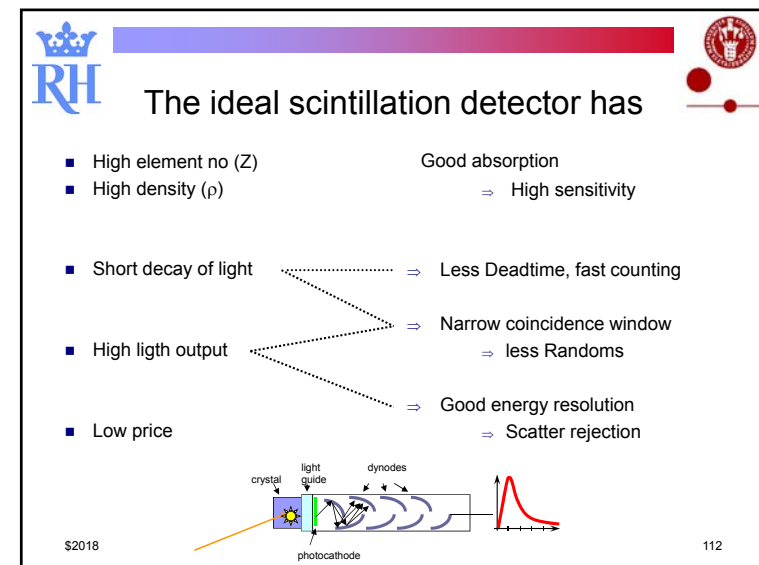
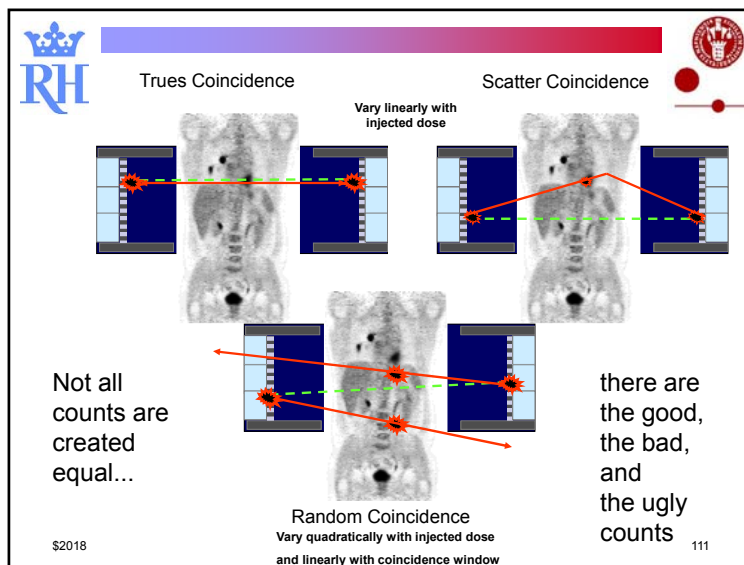
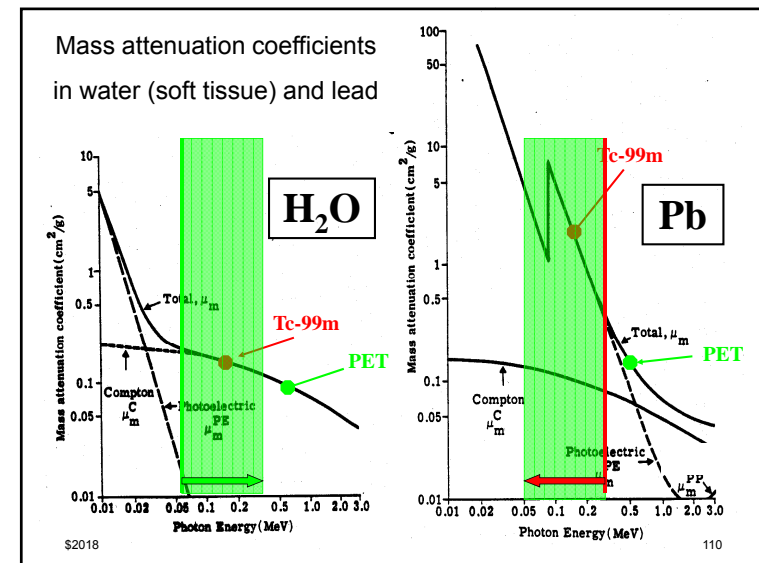
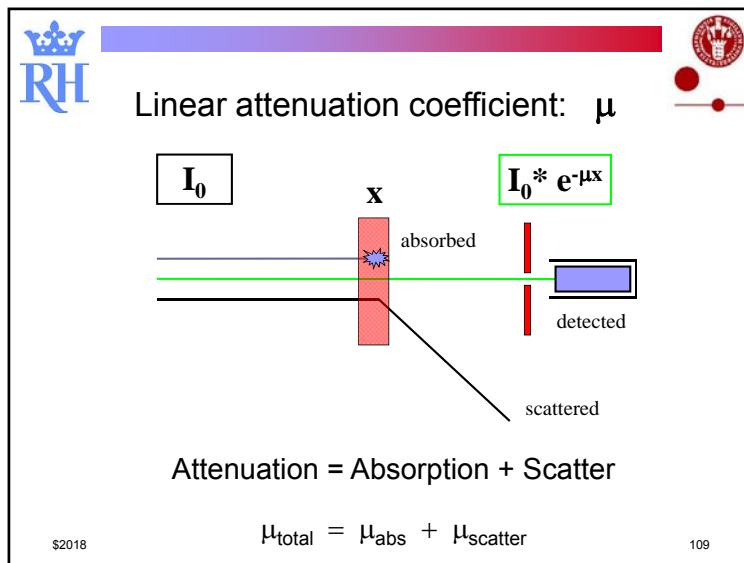
## Physics: definition of attenuation



Monoenergetic, parallel beam of photons

**Attenuation = Absorption + Scatter**

\$2018
108

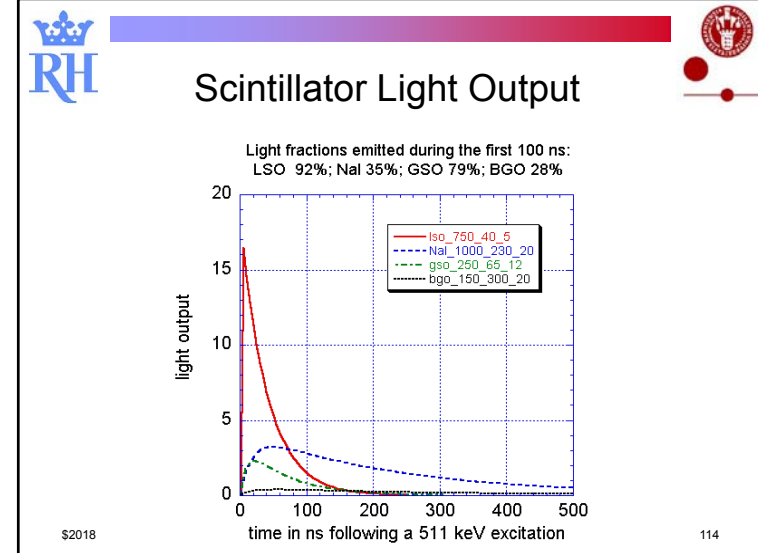


**RH** PET Detector Scintillator Materials

Crystal material	max Z	effective Z	density g/cm <sup>3</sup>	output photons/keV	decay time ns
Nal:TI	53	51	3.7	40	230
BGO	83	73	7.1	8	300
LSO:Ce	71	66	7.4	28	40
LYSO	71	54	5.4	28	53
GSO:Ce	64	59	6.7	7.5	56
BaF <sub>2</sub>	55	54	4.1	2	0.8

"New" promising crystal materials: LaBr<sub>3</sub>, CeBr<sub>3</sub> and TlBr  
BGO may have a come-back

\$2018 113



**RH** Cerenkov photons

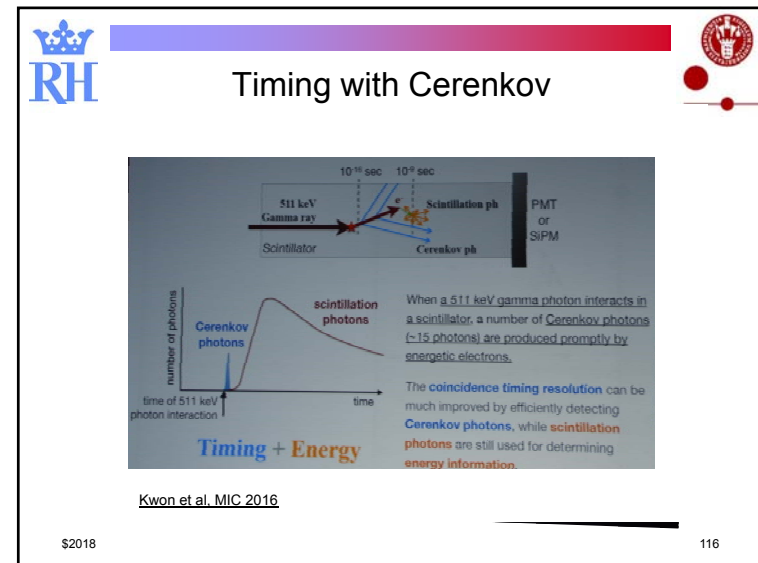
$\cos \theta = \frac{c}{nv}$ 
 $v = \text{particle velocity}$   
 $n = \text{index of refraction of the medium}$

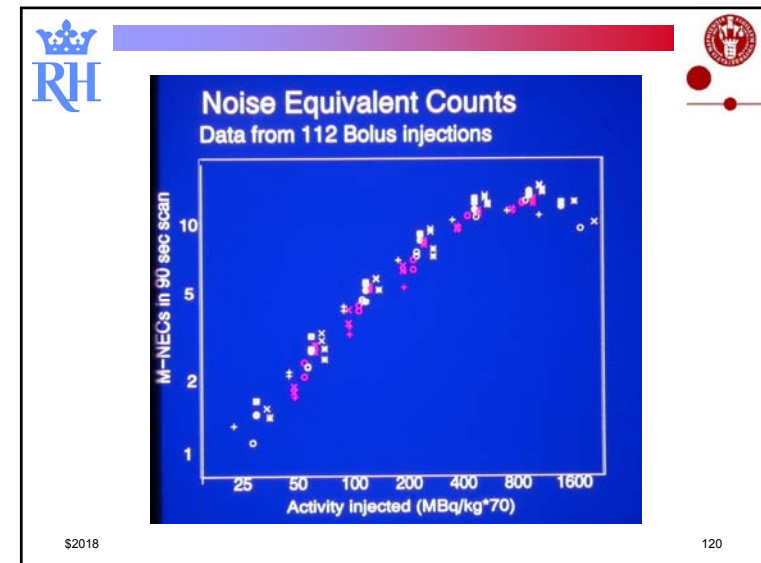
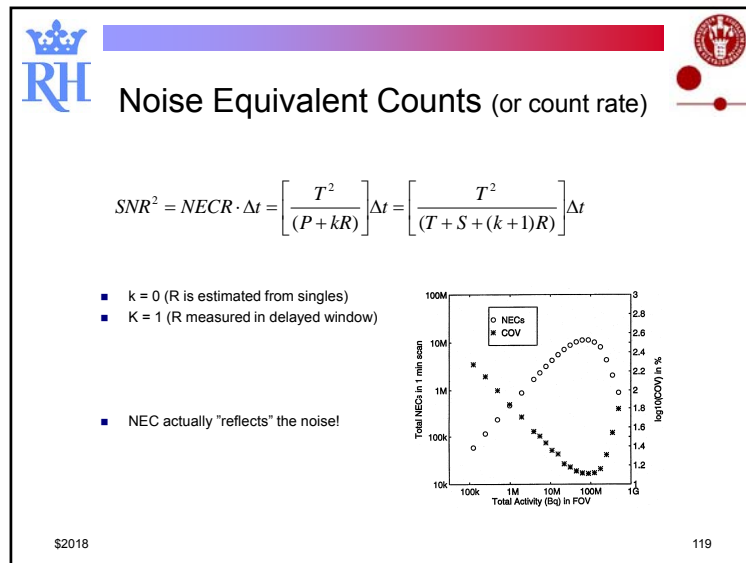
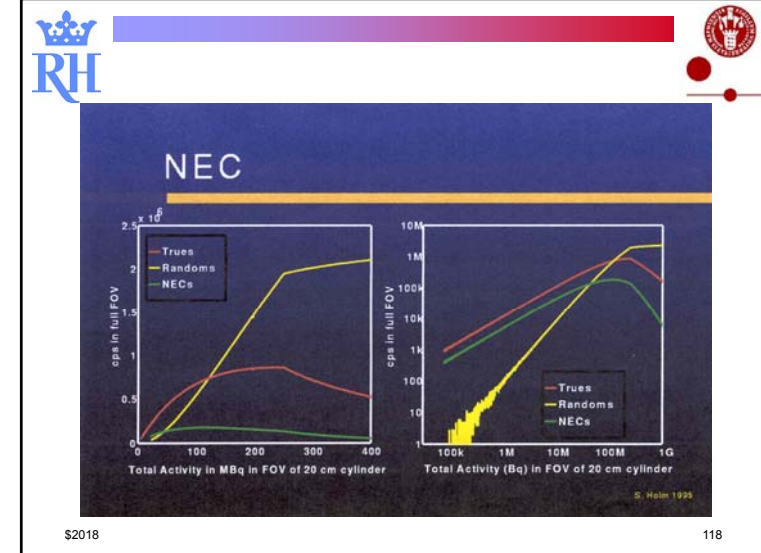
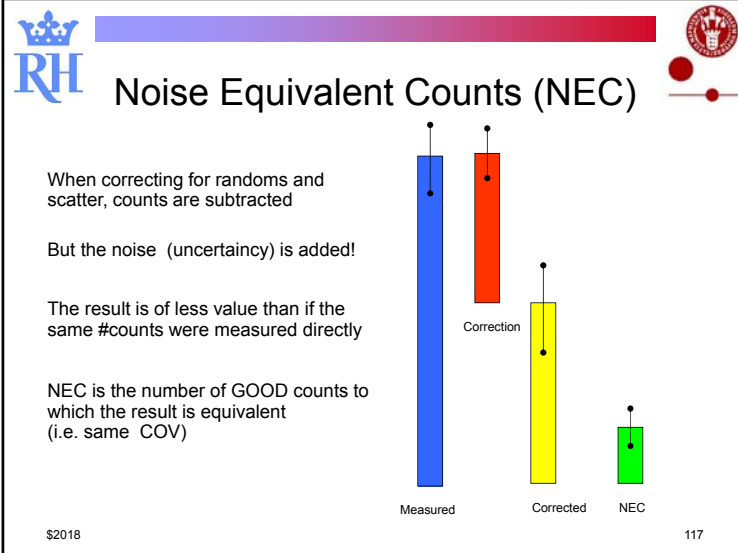
For water with  $n=1.33$ , the limiting angle for high speed particles is given by:  
 $\theta = \cos^{-1} \frac{1}{1.33} = 48.5^\circ$

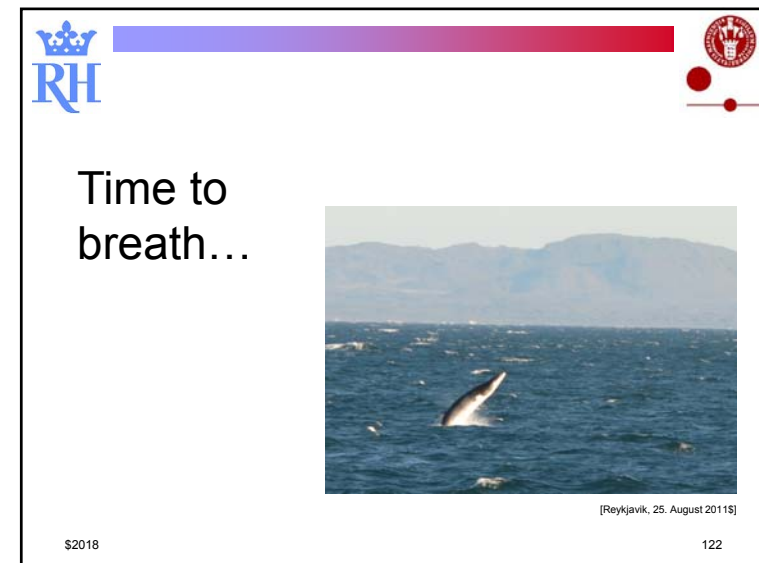
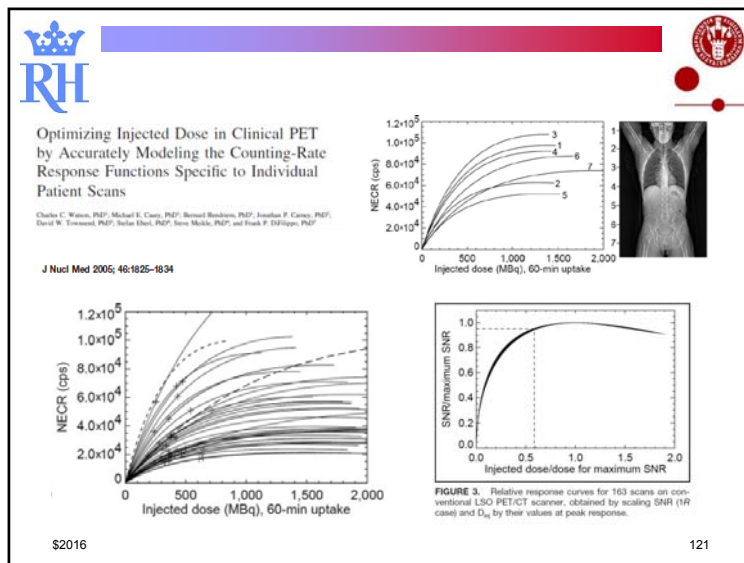
The threshold particle speed for Cerenkov radiation is  $v=c/n$ , which for an electron in water gives a threshold particle kinetic energy of 0.25 MeV.

$\beta = 0.962$ ,  $E_{\text{electron}} = 700 \text{ MeV}$   
 $\frac{1}{\beta^2 - 1} = 1.52$   
 $\frac{1}{\beta^2 - 1} m_0 c^2 = 1.52(0.511 \text{ MeV}) = 770 \text{ MeV}$   
 $Kinetic \text{ energy} = 0.770 \text{ MeV} - 0.511 \text{ MeV} = 0.259 \text{ MeV}$

\$2018 115







**RH**

## Overview (8):

- Different kinds of tomography – PET in particular
- Reconstruction from projections, FBP vs. iterative methods
- Positron imaging history
- Raw data structure - sinograms - types of acquisition and presentation
- 2D/3D, advanced data structure – Michelogram

---

- Resolution and noise
- Scanner physics 1 – PET detectors
- Scanner physics 2 – good, bad, and noise equivalent counts (NEC)
- Attenuation and scatter correction of PET-data
- Hybrid systems – PET/CT- PET/MR - SPECT/CT... Future ideas

\$2018 123

**RH**


## PET is a quantitative technique

(although most people don't care these days...)


IF all the necessary corrections are applied:

- Deadtime
- Geometry, Normalization
- Randoms subtraction
- Attenuation and scatter
- Decay
- ...

\$2018 124

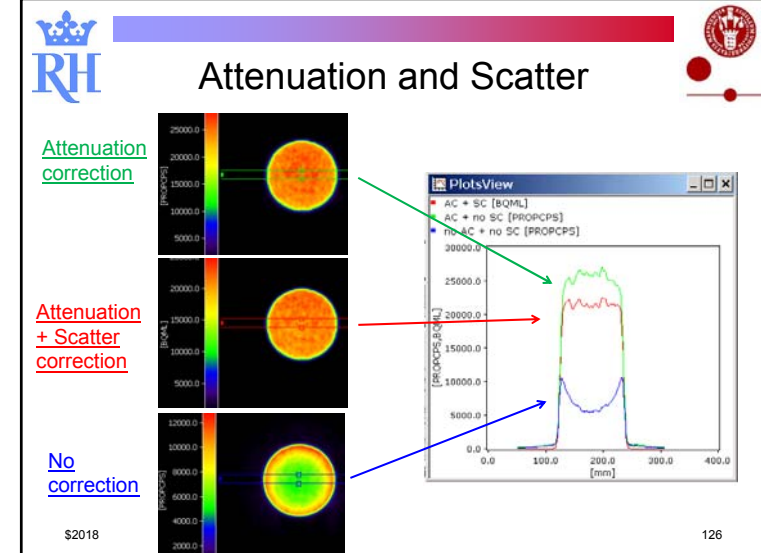



## Attenuation and Scatter




- It is a paradox in our terminology that from a *physics* point of view, **attenuation** (in NM) is caused mainly by **scattering** processes (and only partly by absorption)
- but in our *correction* procedures:
  - **Attenuation** is "lack of counts" that we must restore while
  - **Scatter** is a surplus of counts (in wrong places) to be removed
- Correcting one without the other will give wrong results

\$2018
125

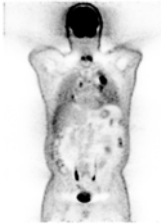


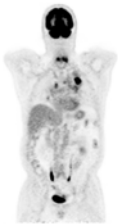


## Attenuation correction



- Provides PET images closer to real radiotracer distribution
- Corrects attenuation-introduced geometric artifacts
- Improves lesion detection in deep organs
- Allows absolute quantitative PET studies



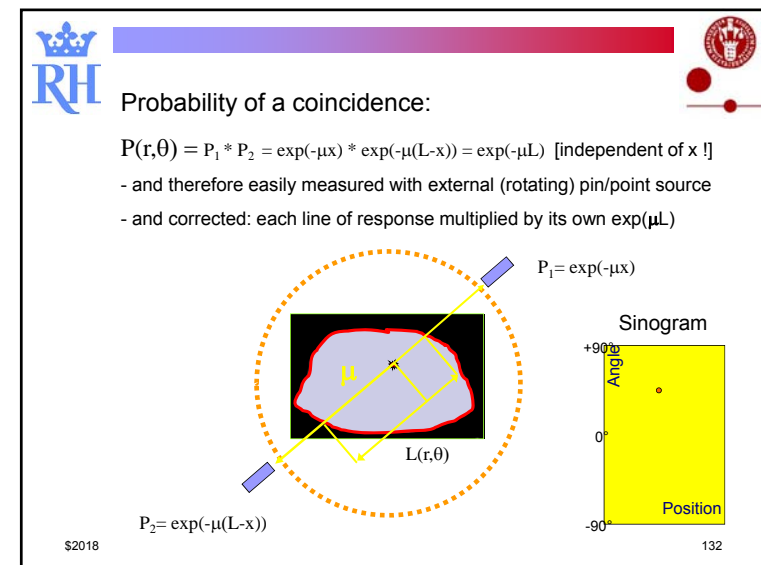
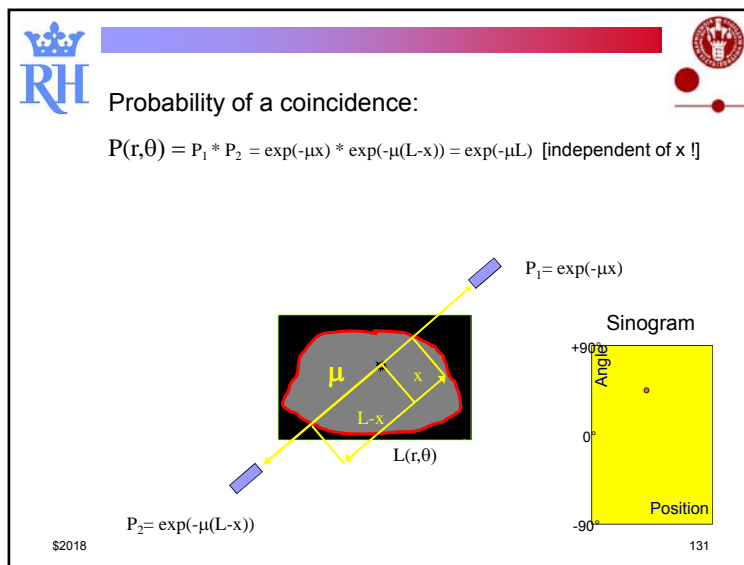
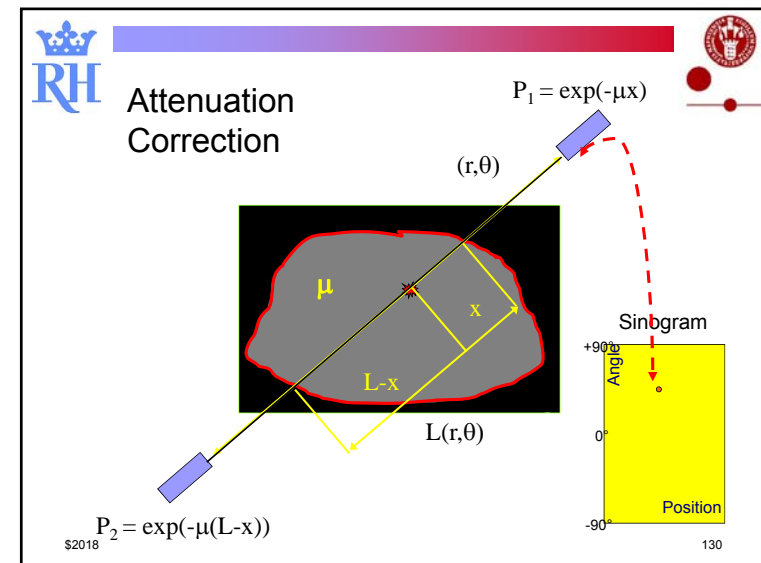
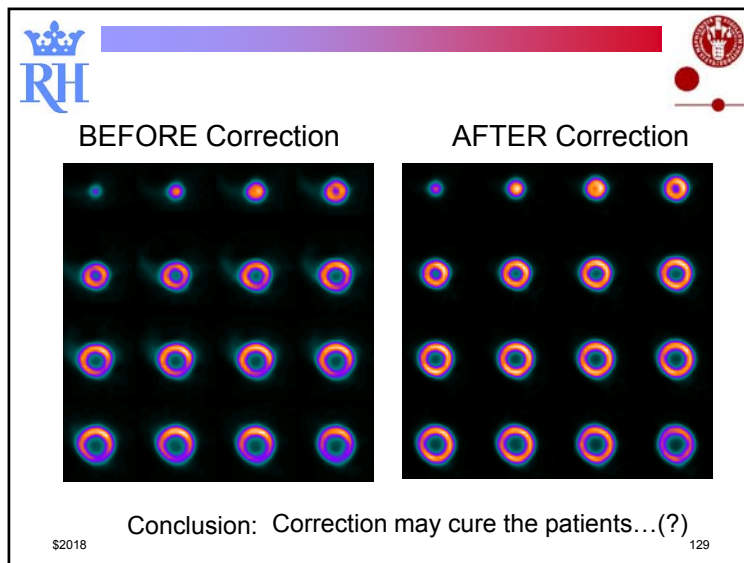


Without attenuation correction
With attenuation correction

\$2018
127



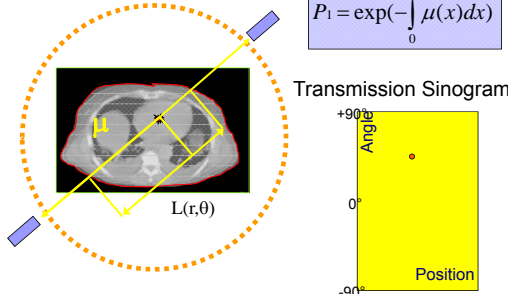




**RH** If  $\mu$  is not a constant (and it IS NOT):

$$P_1 * P_2 = \exp\left(-\int_0^x \mu(x) dx\right) * \exp\left(-\int_x^L \mu(x) dx\right) = \exp\left(-\int_0^L \mu(x) dx\right)$$

still independent of the source position

$$P_1 = \exp\left(-\int_0^x \mu(x) dx\right)$$


Transmission Sinogram

$$P_2 = \exp\left(-\int_x^L \mu(x) dx\right)$$

\$2018

**RH** GE used  $^{68}\text{Ge}$  Pin sources



GE 4096 (by hand)

GE Advance and GE Discovery LS  
(3 pins, automated complex robotic arm)

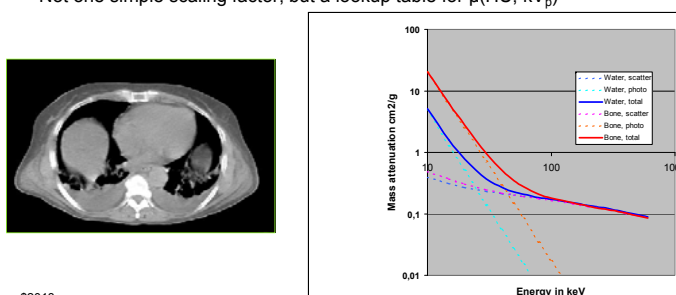
GE Discovery ST etc.  
(1 pin in trunk)

\$2018

134

**RH** CT scans are  $\mu$ -maps (in HU)

They can be used for attenuation correction – essentially noise free  
But:  $\mu(511 \text{ keV}) \neq \mu(80 \text{ keV})$ , therefore a scaling is required  
Soft tissue and bone (and contrast) scale differently  
Not one simple scaling factor, but a lookup table for  $\mu(\text{HU}; \text{kV}_p)$



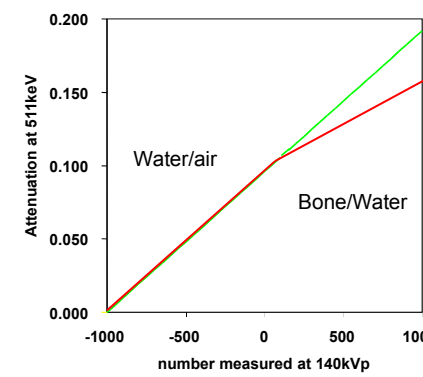
Mass attenuation  $\text{cm}^2/\text{g}$

Energy in keV

\$2018

**RH** Conversion of CT Numbers to  $\mu_{\text{PET}}$

- For CT values  $< 100$ , materials are assumed to have an energy dependence similar to water
- For CT values  $> 100$ , material is assumed to have an energy dependence similar to a mixture of bone and water
- The green line shows the effect of using water scaling for all materials



Attenuation at 511keV

number measured at 140kVp

Water/air

Bone/Water

\$2018

136

**RH** Scatter in SPECT PET

appears "inside" the object      may appear outside object

Crystal Collimator Emission origin Apparent line-of-response

Scatter point Emission origin Field-of-view Apparent line-of-response

\$2018 137

**RH** Scatter Correction by Function Fitting

- Fit data to projection tails
- This requires tails!
- More elaborate methods model the scatter from detailed knowledge of the object

\$2018 138

**RH** Scatter correction techniques

- Metz / Wiener filtering
- Asymmetrical energy window
- Dual energy window
- Dual photopeak window
- Weighing of detected events (WAM)
- Channel ratio method
- Photopeak energy distribution analysis
- Position dependent scatter correction
- Stationary / Non-stationary deconvolution
- Iterative reconstruction techniques
- Neural network
- Pixel by pixel spectral analysis
- Regularized deconvolution-fitting method
- Scatter-free imaging (CFI)
- Holopectral imaging
- Factor analysis of medical image sequences
- **Single scatter simulation techniques**

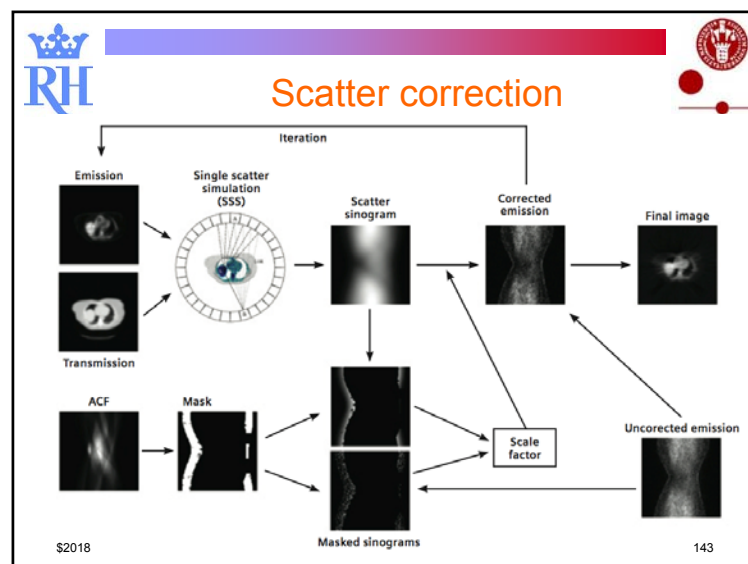
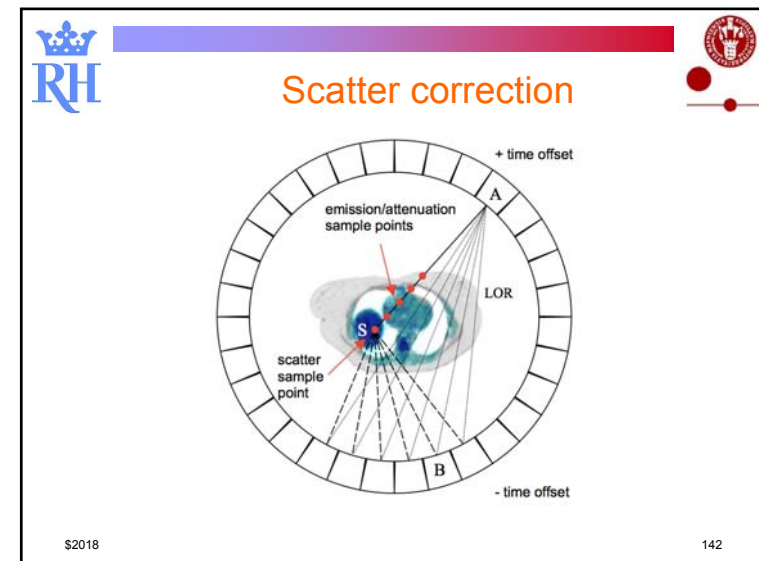
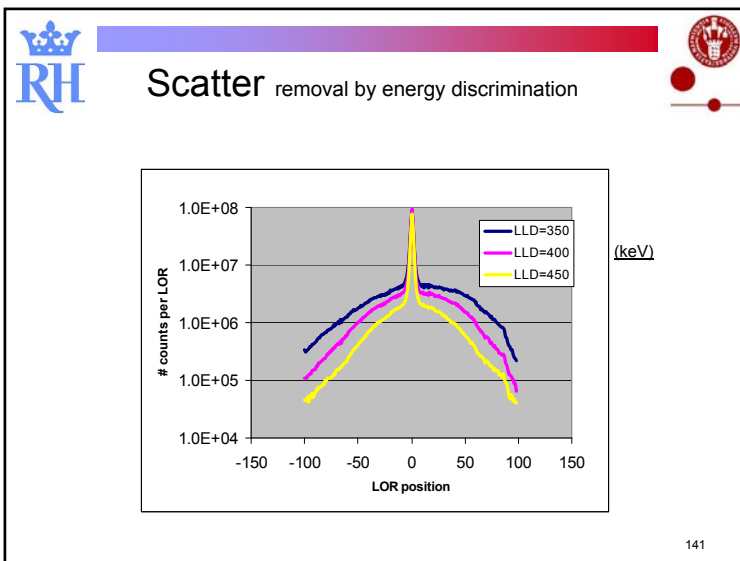
\$2018 139

**RH** Scatter fractions in 3D PET

Brain SF ~ 30-35%

Thorax SF ~ 50-60%

\$2018 140




**RH** Overview (9):


- Different kinds of tomography – PET in particular
- Reconstruction from projections, FBP vs. iterative methods
- Positron imaging history
- Raw data structure - sinograms - types of acquisition and presentation
- 2D/3D, advanced data structure – Michelogram

---

- Resolution and noise
- Scanner physics 1 – PET detectors
- Scanner physics 2 – good, bad, and noise equivalent counts (NEC)
- Attenuation and scatter correction of PET-data
- Hybrid systems – PET/CT- PET/MR - SPECT/CT... Future ideas

144







## Good reasons to combine PET and CT:

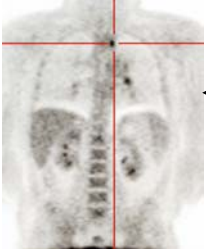
- 0: Because it was possible (*MR more difficult*)
- 1: Complementary information
  - structure + function
  - anatomy + physiologi/biochemistry
- 2: Exact localization ("free" coregistration)
- 3: Improved attenuation correction in PET

\$2018
145

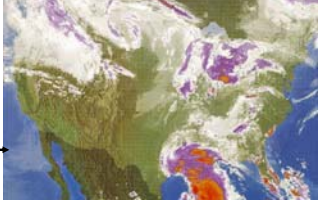





## Functional Images




PET Images  
"abnormal activity"




Weather Patterns  
"weather activity"


 GE imagination at work

\$2018
146







## Structural Images




CT Images  
"precise body's anatomy"




Geographic Map  
"precise outlines of the states"

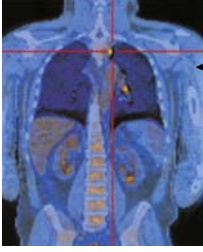
 GE imagination at work

\$2018
147






## Fusion Images



Discovery PET/CT Images  
"abnormal activity **and** precise body's anatomy"



USA Weather Map  
"intense weather **and** precise outlines of the states"

\$2018
148

## PET/CT scanner:

First "physicist's" PET-CT was constructed by Townsend, Beyer, Kinahan et al in Pittsburgh 1994-

We (Rigshospitalet) got a prototype from GE in 2001

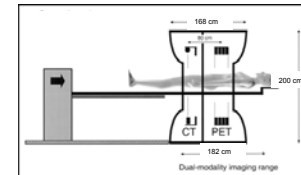
Today commercial devices exist from:

- GE
- Siemens
- Philips
- and a few others
- - with more than 5000 installations worldwide
- Since 2005, almost NO stand-alone PETs have been installed

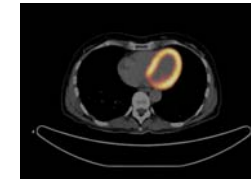
\$2018

149

## PET/CT (or SPECT/CT) scanner:



(Townsend et al 2004)



- combines two modalities in one gantry, common axis, common bed
- allows precise fusion of images
- provides structure + function in the same image
- can use CT for attenuation correction of PET /SPECT)

Anatomical localisation of tracer – Attenuation correction

\$2018

150

## PET/CT: GE Discovery LS

Advance NXI + Lightspeed plus



Detector  
material  
BGO

\$2018

151

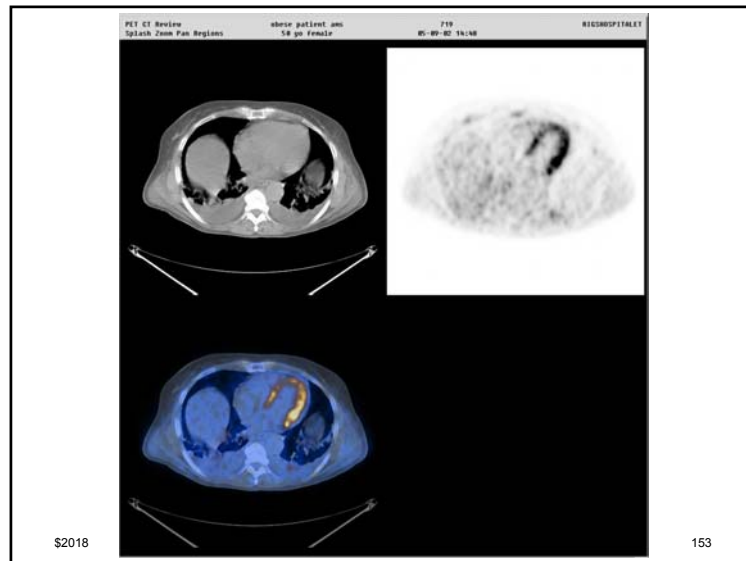
## Inside Discovery LS



\$2018

152





## PET/CT

(images from around 2005)

Herlev  
Hillerød  
Vejle (2)  
Århus Skejby RT

Philips Gemini (KAS Herlev)

Siemens Biograph (RH)

GE Discovery (Milano San Raffaele)

RH (5)  
Næstved (2)  
Århus PET (2)  
Århus NUK  
Herning  
Herlev (3)  
Glostrup

Odense (5)  
Ålborg (2)  
Køge (2)  
Århus Skejby  
Hvidovre  
Gentofte  
Bispebjerg (3)

\$2018

154

## PET/CT instrumentation: adding CT

□ Important design criterion: keeping the patient position (height) stable

(a) CT acquisition

PET acquisition

(b)

PET acquisition

(c)

PET acquisition

\$2018

155

## PET –CT alignment /registration

Not likely to change spontaneously.

For **GE** and **Siemens**: Only opened by service. Must be measured after "invasive procedures"

**Philips Gemini** designed to scan in the separated position also.

\$2018

156




## GE PET – CT alignment





GE Discovery aligns CT with PET transmission using the built-in Ge-68 line sources.

No (other) activity is required  
The phantom contains 5 glass spheres


Newest GE-scanners use similar phantom with Ge-68 spheres



\$2018
157

## Siemens PET – CT alignment





Siemens Biographs have no transmission sources.

Instead 2 Ge-68 line sources mounted in a black box are used.


They are visible on both PET and CT, and an automated algorithm provides the correction

\$2018
158






## Philips PET – CT alignment


- Special service tool holding 6 Na-22 point sources
- Registration performed at 1 year interval



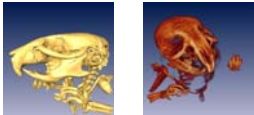
\$2018
159

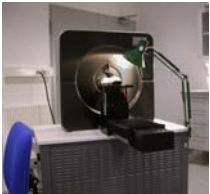



## Small Animal PET-CT




CT resolution down to 15  $\mu$





PET resolution < 2 mm



\$2018
160

**RH** Potential PET-MR configurations

Based on: Eur J Nucl Med Mol Imag (2009) Suppl 1 S86

\$2018 161

**RH** PET-MR: the "easy" solution

\$2018 162

**RH** PET-MR: the "easy" solution

Philips Medical, exhibition RSNA 2012

\$2018 163

**RH** (real) PET-MR is now available

- Siemens made a prototype combination in 2007:
  - 3 T MR scanner with brain coil
  - PET "insert" between coil and magnet
  - Requires detector insensitive to magnetic field
- In 2011, Siemens made an integrated system (APD)
- In 2014, GE followed (SiPM – TOF possible)

\$2018 164




two is now one.



The first whole-body MR-friendly PET architecture

**SIEMENS**

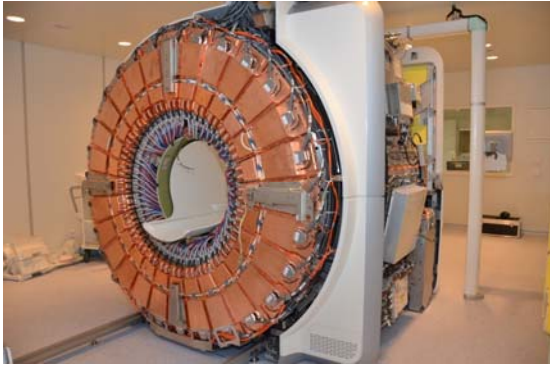


\$2018

165



# PET/MR





All PET electronics is encapsulated in a Faraday cage to avoid RF-interference


\$2018

166

PET(/MR) service (PET module exchange)



\$2018

167









Arrival: 29.November 2011

\$2018

168

**RH**

\$2018      Arrival: 29.November 2011      169

**RH**

Inauguration 14.December 2011

\$2018      170

**RH**

### With PET/CT:

A CT scan is a  $\mu$ -map (expressed in HU)  
 A scaling for energy difference between CT and PET is required  
 Soft tissue and bone (and contrast) scale differently  
 $\Rightarrow$  (only) minor errors in quantitation of PET images

GE Discovery LS (2001)

\$2018      171

**RH**

### In PET/MR:

Attenuation correction is a challenge (and a current research topic)

MR images (in general) are NOT  $\mu$ -maps

Bone, Air, and Metal implants show almost same MR-signal:  $\sim 0$   
 - but they have very different influence on PET attenuation

\$2018      172

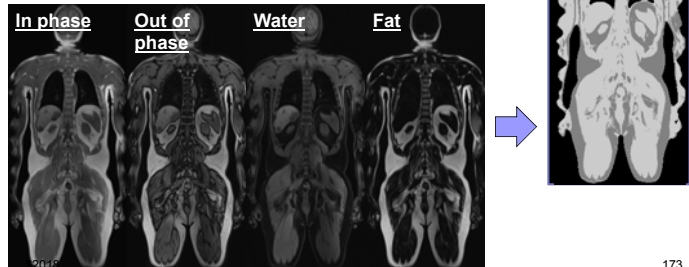


**RH**

## MR-based attenuation correction

Dixon water/fat segmentation (DWFS)  
 \_Martinez-Möller et al., J Nucl Med (2009)

→ Water + Fat + Air + Lung. **No Bone.**

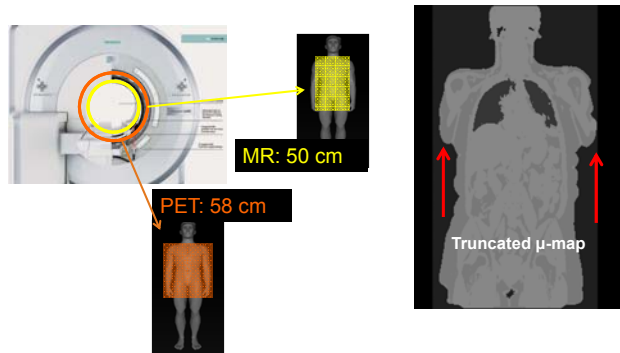


**DWFS  $\mu$ -map**

173

**RH**

Truncation = Mismatch of transverse field-of-view  
 "Arms down" is standard position in PET/MR



MR: 50 cm  
 PET: 58 cm  
 Truncated  $\mu$ -map

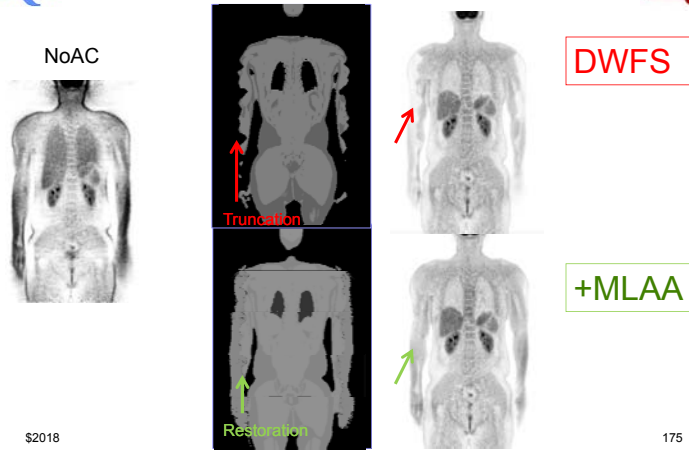
\$2018 [Keller et al. Magnet Reson Mater Phys \(2012\)](#)

174

**RH**

$\mu$ -maps AC-PET

NoAC



Truncation  
 Restoration

DWFS  
 +MLAA

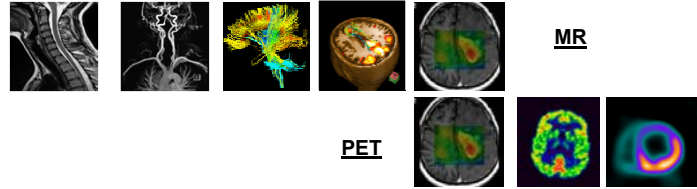
\$2018

175

**RH**

**Vision:**

Morphology, physiology & molecular imaging  
 .....in one scanner ...simultaneously



MR  
 PET

\$2018

176



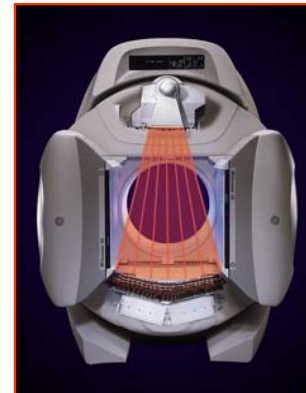
## SPECT/CT

- serves the same dual purpose of Anatomical localisation of tracer and Attenuation correction
- AC is not as simple or "exact" as in PET because we have only one photon
- With CT and iterative recon, quantitation is feasible

\$2018

177

## SPECT/CT (GE Hawkeye)



X-Ray Tube is mounted on the same gantry as the gamma cameras  
A 'CT scan' takes 15 s / cm  
With 1 inch crystals, "PET" is possible



\$2018

178

## SPECT/CT

Siemens



Symbia

\$2018

Philips

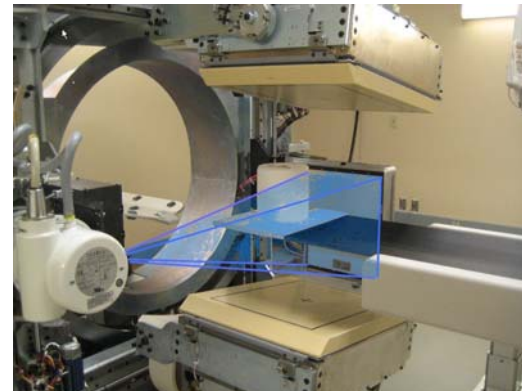


Precedence =

Skylight SPECT + Brilliance CT

179

## BrightView XCT SPECT/CT




\$2018

180

**RH**

## Combinations...

PET-CT / SPECT-CT / PET-MRI / SPECT-MRI



\$2018      Exhibition EANM October 2012      181

**RH**

## PET / SPECT / CT

for small animals



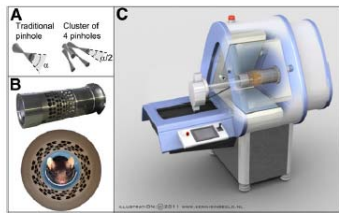
\$2018      182

**RH**

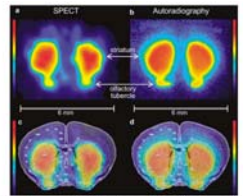
## VECTOR: A Preclinical Imaging System for Simultaneous Submillimeter SPECT and PET

Marlies C. Goorden<sup>a,1</sup>, Frans van der Have<sup>a,1,2</sup>, Rob Kreuger<sup>a</sup>, Ruud M. Ramakers<sup>1,2</sup>, Brendan Vastenhout<sup>1,2</sup>, J. Peter H. Burbach<sup>a</sup>, Jan Booij<sup>a</sup>, Carla F.M. Molthoff<sup>a</sup>, and Freck J. Beekman<sup>1,2</sup>

J Nucl Med 2013; 54:306-312  
DOI: 10.2967/jnumed.112.109538



**FIGURE 1.** Integration of clustered-pinhole collimator into existing SPECT/CT platform. (A) Traditional pinhole with opening angle  $\alpha$  and cluster of 4 pinholes with approximately same field of view and opening angle  $\alpha/2$ . (B) Clustered-pinhole collimator optimized for imaging SPECT and PET tracers, into which mouse is placed. (C) Collimator mounted in SPECT/CT system.



**Figure 2.** High resolution in vivo imaging of renal DMSO (left) compared with SPECT autoradiography (right).

\$2018      183

**RH**      **MI Labs**

## G-SPECT

• Game-Changing SPECT



\$2018      184



## Spectrum Dynamics D-SPECT



CZT  
= CdZnTe

\$2018

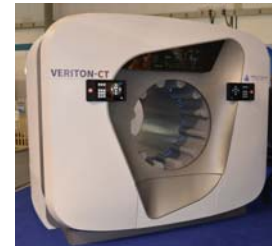
185



## Spectrum Dynamics Veriton-CT



CZT = CdZnTe



\$2018

186



## PET / SPECT / CT



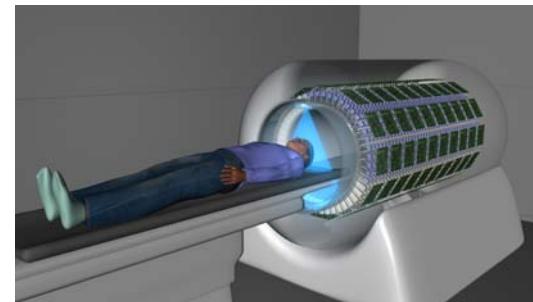
AnyScan  
Mediso  
Budapest

Exhibition at  
EANM 2008  
Still marketed



\$2018

187



UCDAVIS  
UNIVERSITY OF CALIFORNIA

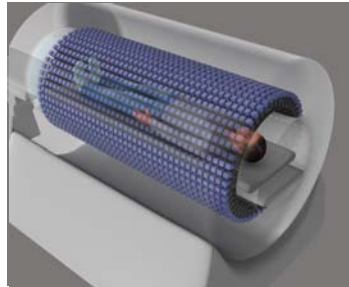
\$2018



Penn  
UNIVERSITY OF PENNSYLVANIA

188

## Maximizing Sensitivity by Total-Body PET



- ~40-fold increase**  
for adult total-body imaging
- ~20-fold increase**  
for pediatric total-body imaging
- ~4-fold increase**  
for single organ imaging

\$2018

189

## Applications

### Systemic disease and therapies:

- Cancer: Ultra-staging and micrometastasis
- Inflammation
- Infection
- Cellular therapy and trafficking
- Mind-body interactions

### Total body pharmacokinetics

- Drug development
- Toxicology
- Biomarker discovery

### Low dose opens up new populations:

- Expanded use in pediatrics
- Use in chronic disease
- Studies of normal biology



\$2018

190

## Completed EXPLORER Scanner

### System:

Ring diameter: 78.6 cm  
Transaxial FOV: 68.6 cm  
Axial FOV: 194.8 cm

# of crystals: 564,480  
# crystal blocks: 13,440  
# of SiPMs: 53,760

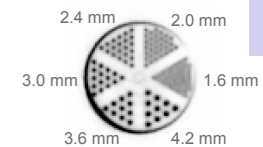
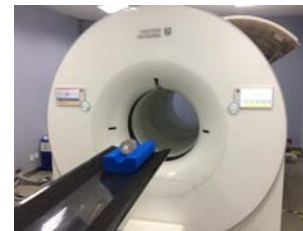
80 detector row CT



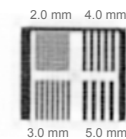
\$2018

191

## Preliminary Resolution Tests



mini Derenzo:  
8 billion prompts  
transaxial slice



axial bar:  
12 billion prompts  
sagittal slice

\$2018

192



# J-PET

Longitudinal plast-scintillators

P Moskal *et al*  
Phys. Med. Biol. **61** (2016) 2025

\$2018

193

UNIVERSITY OF COPENHAGEN
RIGSHOSPITALET

# Advances in Dynamic Radioactive Scanning

Compiled and Edited by  
YEN WANG, M.D., D.Sc. (MED.)  
Associate Professor of Radiology  
University of Pittsburgh  
and  
Chairman, Department of Radiology  
Homestead Hospital  
Pittsburgh, Pennsylvania

CHARLES C THOMAS • PUBLISHER  
Springfield • Illinois • U.S.A.

# 1968 PET

\$2018

194

UNIVERSITY OF COPENHAGEN
RIGSHOSPITALET

# 1966

# 2015

Development of the Helmet-Chin PET Prototype

Hidetaka Tachikawa, Eiji Yoshida, Fumihiko Nishikubo, Hidetaka Wakatsuki, Masamichi Nitta, Akiko M. Akino,  
Akira Matsuoka, Shiroki Tazawa, Yuzuru Kaneko, Tetsuo Ishida, Yoshiko Fujiwara,  
and Togo Tazawa, Shimizu, 2015

Chiba, Japan [Poster M3CP-97 at MIC2015]

Fig. 1. Photograph of the first prototype of the helmet-chin PET (a), design sketch (b), and geometry of the crystals (c), (d).

1966rBrookhaven 1966 – moved to MNI 1968

UNIVERSITY OF COPENHAGEN
RIGSHOSPITALET

# 1960

# 2015

Development of the Helmet-Chin PET Prototype

Hidetaka Tachikawa, Eiji Yoshida, Fumihiko Nishikubo, Hidetaka Wakatsuki, Masamichi Nitta, Akiko M. Akino,  
Akira Matsuoka, Shiroki Tazawa, Yuzuru Kaneko, Tetsuo Ishida, Yoshiko Fujiwara,  
and Togo Tazawa, Shimizu, 2015

Chiba, Japan [Poster M3CP-97 at MIC2015]

Fig. 1. Photograph of the first prototype of the helmet-chin PET (a), design sketch (b), and geometry of the crystals (c), (d).

\$2018

196

### Could this become a "trend" ?

**IF** a cure for, e.g. Alzheimer's disease is found

**AND**

**IF** we have a PET-tracer that can tell if that cure works for YOU

**AND**

**IF** this device can be manufactured for  $\frac{1}{4}$  of the price of WB PET/CT

**THEN** it is likely to.

Time to  
press...

